

Equilibrium and off-equilibrium trap-size scaling in 1D ultracold bosonic gases

Massimo Campostrini and Ettore Vicari

*Dipartimento di Fisica dell'Università di Pisa and I.N.F.N.,
Sezione di Pisa, Largo Bruno Pontecorvo 2, I-56127 Pisa, Italy*

(Dated: October 9, 2010)

We study some aspects of equilibrium and off equilibrium quantum dynamics of dilute bosonic gases in the presence of a trapping potential. We consider systems with a fixed number of particles and study their scaling behavior with increasing the trap size.

We focus on one-dimensional (1D) bosonic systems, such as gases described by the Lieb-Liniger model and its Tonks-Girardeau limit of impenetrable bosons, and gases constrained in optical lattices as described by the Bose-Hubbard model. We study their quantum (zero-temperature) behavior at equilibrium and off equilibrium during the unitary time evolution arising from changes of the trapping potential, which may be instantaneous or described by a power-law time dependence, starting from the equilibrium ground state for an initial trap size.

Renormalization-group scaling arguments, analytical and numerical calculations show that the trap-size dependence of the equilibrium and off-equilibrium dynamics can be cast in the form of a trap-size scaling in the low-density regime, characterized by universal power laws of the trap size, in dilute gases with repulsive contact interactions and lattice systems described by the Bose-Hubbard model. The scaling functions corresponding to several physically interesting observables are computed.

Our results are of experimental relevance for systems of cold atomic gases trapped by tunable confining potentials.

PACS numbers: 67.85.-d, 05.30.Jp, 67.85.Hj, 05.30.Rt

I. INTRODUCTION

The dynamics of strongly correlated quantum systems is a fundamental physical issue which has attracted much theoretical interest. The achievement of Bose-Einstein condensation in dilute atomic vapors [1] and the impressive progress in the experimental manipulation of cold atoms in optical lattices, see, e.g., Ref. [2] and references therein, have provided a great opportunity to investigate the interplay between quantum and statistical behaviors in particle systems, and issues related to the unitary quantum evolution of closed many-body systems, exploiting their low dissipation rate which allows to maintain phase coherence for a long time. Transitions between different quantum phases have been experimentally observed, such as those related to the formation of a Bose-Einstein condensate in interacting Bose gases [3–5] and quantum Mott-insulator to superfluid transitions in atomic systems constrained in optical lattices, see, e.g., Refs. [6–11]. Accurate experimental studies of nonequilibrium properties of quantum many-body systems of ultracold atoms have also been reported, see, e.g., Refs. [12–14].

An important feature of these experiments is the presence of a confining potential which traps the particles within a limited spatial region. The capability of varying the confining potential, which may also depend on the spatial directions, allows to vary the effective spatial geometry of the particle systems, including quasi-1D geometries, see, e.g., Refs. [13, 15–19].

In the presence of an optical lattice with lattice spacing a , created by laser-induced standing waves which constrains the particle to stay at the sites of a lattice, the the-

oretical framework [20] is provided by the Bose-Hubbard (BH) model [21] with a confining potential $V(r)$ coupled to the particle density, defined by the Hamiltonian ¹

$$\mathcal{H}_{\text{BH}} = \frac{J}{2} \sum_{\langle ij \rangle} (b_j - b_i)^\dagger (b_j - b_i) + \frac{U}{2} \sum_i n_i (n_i - 1) + \sum_i V(r_i) n_i, \quad (1)$$

where $\langle ij \rangle$ is the set of nearest-neighbor sites, b_i are bosonic operators, $n_i \equiv b_i^\dagger b_i$ is the particle density operator, and $N = \langle \sum_i n_i \rangle$ is the particle number. We consider a power-law spatial dependence for the trapping potential,

$$V(r) = \frac{1}{p} v^p r^p, \quad (2)$$

where $r \equiv |\vec{x}|$ is the distance from the center of the trap, v is a positive constant and p an even integer number. Experiments are usually set up with a harmonic potential, i.e., $p = 2$. Examples of experimental traps described by quartic potentials are reported in Ref. [22]. The hard-core (HC) limit $U \rightarrow \infty$ of the BH model implies that the particle number n_i per site is restricted to the values $n_i = 0, 1$. In one dimension the HC limit can be

¹ The BH Hamiltonian for N particles is usually written with the kinetic term $\mathcal{H}_{\text{kin}} = -(J/2) \sum_{\langle ij \rangle} (b_j^\dagger b_i + b_i^\dagger b_j)$. The difference from Eq. (1) is a N -dependent constant.

exactly mapped into a lattice model of spinless fermions, see, e.g., Ref. [23].

We consider

$$l \equiv \frac{J^{1/p}}{v} \quad (3)$$

as the size of the trap within the confined BH model [24, 25]. In the case of harmonic traps, $l \sim \omega^{-1}$ where ω is the trap frequency. The definition (3) of trap size naturally arises when we consider the *thermodynamic* limit, which is generally defined as $N, l \rightarrow \infty$ keeping N/l^d fixed [2, 26], and it is equivalent to introducing a chemical potential μ , adding the term $\mu \sum_i n_i$ to the Hamiltonian (1).

In the absence of a lattice structure, the basic model to describe the many-body features of a boson gas confined to an effective 1D geometry is the Lieb-Liniger (LL) model with an effective two-particle repulsive contact interaction [27],

$$\mathcal{H}_{\text{LL}} = \sum_{i=1}^N \left[\frac{p_i^2}{2m} + V(x_i) \right] + g \sum_{i \neq j} \delta(x_i - x_j) \quad (4)$$

where N is the number of particles and $V(x)$ is the confining potential. The limit of infinitely strong repulsive interactions corresponds to a 1D gas of impenetrable bosons [28, 29], the Tonks-Girardeau (TG) gas. 1D Bose gases with repulsive two-particle short-ranged interactions become more and more nonideal with decreasing the particle density, acquiring fermion-like properties, so that the 1D gas of impenetrable bosons is expected to provide an effective description of the low-density regime [30]. 1D Bose gases of cold atoms have been realized experimentally [13, 15, 17–19].

In this paper we address issues related to the equilibrium and off equilibrium quantum dynamics of dilute bosonic gases in the presence of a confining potential. We consider 1D trapped gases constituted by N bosonic particles, at the equilibrium and off equilibrium during the unitary time evolution arising from changes of the trapping potential. In the latter case we consider a system of N particles in a trap of size l_0 , which is prepared in its ground state at $t = 0$, the trapping potential is then varied as

$$V(r, t) = \frac{1}{p} u^p K(t/t_q) r^p, \quad (5)$$

with $K(0) = 1$ and the parameter t_q providing the time rate of the variation of the trapping. Since the particle number $\hat{N} \equiv \sum_x n_x$ commutes with the time-dependent Hamiltonian even when the trapping potential depends on the time, the particle number N remains unchanged during the dynamical process. Instantaneous changes from the initial trap size $l_0 \equiv 1/u$ to a final trap size l_f , or a complete drop of the trap (corresponding to $l_f \rightarrow \infty$), give rise to interesting cases of off-equilibrium evolutions.

Moreover, we also consider a power-law time dependence of the confining potential such as

$$K(t/t_q) = \tau^q, \quad \tau \equiv 1 + t/t_q. \quad (6)$$

Adiabatic time evolutions apply when the change of the external potential is very slow, thus it requires a large time rate $|t_q|$.

Several theoretical studies have already been dedicated to issues related to the quantum behavior of trapped bosonic gases, in the continuum and on the lattice (i.e., the BH model), in equilibrium conditions and off equilibrium due to time-variations of the trapping potential, see, e.g., Refs. [2, 24–26, 31–58].

In this paper we further investigate these issues within the framework of the trap-size scaling (TSS) theory [25, 59]. We consider systems with a fixed number of particles N and study their scaling behavior with increasing the trap size l . We study the asymptotic trap-size dependence in the low-density regime which is characterized by universal power laws, as we shall see.

Using renormalization-group (RG) scaling arguments, we derive the power-law behaviors which describe the asymptotic TSS in the low-density regime at equilibrium. They are determined by the continuum *nonrelativistic* bosonic Φ^4 theory, which is the same continuum theory describing the quantum critical behavior at Mott transitions driven by the chemical potential [21]. This implies that in one and two dimensions the power-law TSS is characterized by the dynamic exponent $z = 2$, the RG dimensions $y_b = d/2$ and $y_n = d$ of the bosonic and particle density operators respectively [21, 23], and the trap exponent $\theta = p/(p+2)$ [25]. This general TSS scenario is supported by analytical and numerical calculations within 1D systems. We show that the TSS is universal for diluted gases with repulsive contact interactions such as the LL model (4) and lattice systems described by the BH model (1).

We consider the off-equilibrium behavior arising from time variations of the confining potentials, which may be instantaneous or described by a power-law time dependence, such as Eq. (6), starting from the equilibrium ground state for an initial trap size l_0 . We put forward scaling Ansatz for the asymptotic TSS with respect to the initial trap size l_0 in the large- l_0 limit. Then we study the trap-size dependence of the off-equilibrium dynamics of 1D bosonic gases of N particles, by assuming an adiabatic evolution in the case of slow changes of the Hamiltonian parameters, and by analyzing the solutions of the Schrödinger equation of N impenetrable bosons in the presence of time-dependent harmonic potentials.

Our results are of experimental relevance for systems of cold atomic gases trapped by tunable confining potentials. Indeed, the long characteristic time scales of these systems may allow a scaling study of the trap-size dependence of the zero-temperature properties of N -particle boson gases in the low-density regime, at equilibrium and off equilibrium during the time evolution of the confining potential.

The paper is organized as follows. In Sec. II we derive the asymptotic TSS of bosonic systems of N particles at equilibrium in the large trap-size limit, using general scaling arguments. In Sec. III we focus on the 1D BH model, we present analytical and numerical calculations in the HC limit and at finite U , which support the RG scaling predictions, and provide the universal scaling functions at equilibrium. In Sec. IV we consider 1D bosonic gases at low density, and, in particular, in the TG limit which describes the low-density behavior of the LL model: we show that the trap-size dependence of N -particle systems is identical to the asymptotic TSS of the 1D BH model with the same number of particles. In Sec. V we turn to off-equilibrium dynamics, considering time-dependent confining potentials or instantaneous changes of its parameters; using scaling arguments we extend the equilibrium TSS Ansatz to the case of the off-equilibrium evolutions, distinguishing the cases of instantaneous variations and power-law time dependences of the confining potential. In Sec. VI we discuss the case of slow time variations of the trapping potential, assuming an adiabatic or quasi-adiabatic approximation. Sec. VII is dedicated to the study of the quantum unitary evolution of 1D impenetrable bosons in time-dependent harmonic traps, where the off-equilibrium trap-size dependence can be analytically determined, in particular, for a linear time-dependence of the confining potential and for instantaneous quenches. Finally, in Sec. VIII we summarize our main results and draw our conclusions. In App. A we discuss the case of particle systems confined by a spatial dependence of the hopping parameter. In App. B we study the asymptotic behavior of the TSS functions for a large number of particles, showing that they have a nontrivial large- N power-law scaling. App. C presents a detailed analysis of the off-equilibrium dynamics of a quantum oscillator with a time-dependent frequency.

II. TRAP-SIZE SCALING OF N PARTICLES AT EQUILIBRIUM

Before discussing the TSS of N particles in the large- l limit, let us note that the large- l limit keeping N fixed differs from that performed at fixed chemical potential μ , i.e., considering the BH Hamiltonian

$$\mathcal{H}_\mu = \mathcal{H}_{\text{BH}} + (\mu - J) \sum_i n_i. \quad (7)$$

Indeed, the large trap-size limit, keeping μ fixed, implies an increase of the particle number so that

$$N/l^d = \tilde{\rho}(\mu/J) \quad (8)$$

asymptotically, where d is the spatial dimension and $\tilde{\rho}(\mu)$ is a finite function of μ . This *thermodynamic* limit is usually considered when quantum transitions are studied in confined particle systems, see, e.g., Ref. [55].

We are interested in the low-density regime, which is related to the limit $\mu \rightarrow \mu_c$ where $\tilde{\rho}(\mu_c) = 0$, which corresponds to a low-density to empty-state transition, which may be considered as a $n = 0$ Mott transition. In the homogeneous BH model without trap, the low-energy properties at Mott transitions driven by the chemical potential μ are described by a *nonrelativistic* U(1)-symmetric bosonic Φ^4 field theory [21], whose partition function is given by

$$Z = \int [D\phi] \exp \left(- \int_0^{1/T} dt d^d x \mathcal{L} \right), \quad (9)$$

$$\mathcal{L} = \phi^* \partial_t \phi + \frac{1}{2m} |\nabla \phi|^2 + r |\phi|^2 + u |\phi|^4,$$

where $r \sim \mu - \mu_c$. The upper critical dimension of this bosonic theory is $d = 2$, thus its critical behavior is of mean-field type for $d > 2$. For $d = 2$ the field theory is essentially free (apart from logarithmic corrections), thus the dynamic critical exponent is $z = 2$ and the RG dimension of the coupling μ is $y_\mu = 2$. In $d = 1$ the theory turns out to be equivalent to a free field theory of nonrelativistic spinless fermions, thus $z = 2$ and $y_\mu = 2$ as well, see, e.g., Ref. [23].

The quantum critical behaviors in the presence of the trapping potential can be described in the theoretical framework of the TSS theory [25], which introduces a trap critical exponent θ which describes how the length scale at the quantum critical point diverges with increasing the trap size l , i.e., $\xi \sim l^\theta$ [59]. The trap exponent at the Mott transitions of 1D and 2D BH models is

$$\theta = p/(p+2). \quad (10)$$

At the low-density to empty-state transition the TSS of the free-energy density in the presence of a confining potential (2) is given by [25, 55]

$$F(\mu, T, l, x) = l^{-\theta(d+z)} \mathcal{F}(\bar{\mu} l^{\theta/\nu}, T l^{\theta z}, x l^{-\theta}), \quad (11)$$

where x is the distance from the middle of the trap, T is the temperature, $\bar{\mu} \equiv \mu - \mu_c$, and $\nu \equiv 1/y_\mu$. The zero-temperature TSS of a generic observable, whose low-density critical behavior is described by the RG dimension y_o in the homogeneous system, is given by

$$\langle O \rangle(\mu, l, x) \sim l^{-y_o \theta} \mathcal{O}(\bar{\mu} l^{\theta/\nu}, x l^{-\theta}). \quad (12)$$

For example, any low-energy scale at $T = 0$ is expected to behave as $E = l^{-z\theta} \mathcal{E}(\bar{\mu} l^{\theta/\nu})$; the particle density as $\langle n_x \rangle = l^{-d\theta} \mathcal{D}(\bar{\mu} l^{\theta/\nu}, x l^{-\theta})$ (using the fact that the RG dimension of the density operator is $y_n = d$); the one-particle density matrix as

$$\rho_1(x, y) = \langle b_x^\dagger b_y \rangle = l^{-d\theta} \mathcal{M}(\bar{\mu} l^{\theta/\nu}, x l^{-\theta}, y l^{-\theta}), \quad (13)$$

using the fact that $y_b = d/2$; etc....

The limit $\bar{\mu} \rightarrow 0$ corresponds to the low-density regime $N a^d / l^d \rightarrow 0$ where a is the lattice spacing. A TSS Ansatz

for the large- l trap-size dependence at fixed particle number N can be derived by replacing the dependence on $\bar{\mu}l^{\theta/\nu}$ with that on N . See also the next section for an explicit derivation in 1D systems. Therefore, for a generic observable we expect

$$\langle O \rangle(N, l, x) \sim l^{-y_o\theta} \mathcal{O}_N(xl^{-\theta}). \quad (14)$$

In particular, the gap, i.e., the energy difference of the lowest states, behaves as

$$\Delta_N \approx A_N l^{-z\theta}, \quad (15)$$

where A_N is a N -dependent amplitude. Since the RG dimension of the particle density operator n_i is given by $y_n = d + z - y_\mu = d$, we expect that

$$\rho(x) \equiv \langle n_x \rangle \approx l^{-d\theta} \mathcal{D}_N(X), \quad (16)$$

and

$$G_n(x, y) \equiv \langle n_x n_y \rangle - \langle n_x \rangle \langle n_y \rangle \approx l^{-2d\theta} \mathcal{G}_N(X, Y), \quad (17)$$

where $X = x/l^\theta$ and $Y = y/l^\theta$, and the scaling functions \mathcal{D}_N and \mathcal{G}_N depend on N . The RG dimension of the boson operator is $y_b = d/2$, thus the low-density TSS of the one-particle density matrix is

$$\rho_1(x, y) \equiv \langle b_x^\dagger b_y \rangle \approx l^{-d\theta} \mathcal{M}_N(X, Y). \quad (18)$$

Finally, we consider the momentum distribution, defined as

$$n_k \equiv \frac{1}{N} \sum_{x, y} e^{ik(x-y)} \rho_1(x, y), \quad (19)$$

normalized so that $\int \frac{dk}{2\pi} n_k = 1$. n_k is usually accessible experimentally from the interference patterns of absorption images taken after the drop of the trap and the expansion of the atomic gas. Eq. (18) implies

$$n_k \approx l^{\theta(2-d)} \mathcal{N}_N(K), \quad K = l^\theta k. \quad (20)$$

In the next sections we report analytic and numerical calculations for the BH model and a gas of impenetrable bosons, showing that they share the same asymptotic TSS behavior, with the same scaling functions.

III. TRAPPED PARTICLES AT EQUILIBRIUM ON A 1D LATTICE

In this section we address issues related to the equilibrium properties of a 1D lattice system of N bosonic particles confined by a trapping potential, described by the 1D BH model (1). These results will also be relevant for the off-equilibrium evolution of the system under variations of the confining potential, in particular when the dynamics is so slow to admit the adiabatic approximation. In the following we set the hopping parameter $J = 1$, thus the trap size (3) simply becomes $l = 1/v$.

To complete the definition of the BH model in the presence of the confining potential, we consider traps whose center coincides with a site of the lattice, so that the lattice model has a reflection symmetry with respect to the center of the trap. However, any other particular choice, i.e., centering the trap anywhere between two sites, does not change the asymptotic low-density TSS behavior, leading to an effective asymptotic reflection symmetry.

A. The hard-core limit

We first consider the hard-core (HC) limit $U \rightarrow \infty$ of the 1D BH model, which allows us to study the effects of the confining potential by exact and very accurate numerical results. The HC limit implies that the particle number n_i per site is restricted to the values $n_i = 0, 1$. In this limit the 1D BH model (7) can be mapped into the XX chain model with lattice spacing a and a space-dependent transverse external field,

$$H_{\text{XX}} = - \sum_i (S_i^x S_{i+1}^x + S_i^y S_{i+1}^y) - \sum_i [\mu + V(x_i)] S_i^z, \quad (21)$$

where $S_i^a = \sigma_i^a/2$ and σ_i^a are the Pauli matrices, which are related to the boson operators b_i by $\sigma_i^x = b_i^\dagger + b_i$, $\sigma_i^y = i(b_i^\dagger - b_i)$, $\sigma_i^z = 1 - 2b_i^\dagger b_i$. Then, by a Jordan-Wigner transformation, one can further map it into a model of spinless fermions, see, e.g., Ref. [23], with a quadratic Hamiltonian

$$H_q = \sum_{ij} c_i^\dagger h_{ij} c_j + (\mu - 1) \sum_i c_i^\dagger c_i, \quad (22)$$

where c_i is a spinless fermion operator, and

$$h_{ij} = \delta_{ij} - \frac{1}{2}\delta_{i,j-1} - \frac{1}{2}\delta_{i,j+1} + V(x_i)\delta_{ij}. \quad (23)$$

Issues related to quantum transitions in particle systems are best discussed in the presence of the chemical potential μ . In the absence of the trap, the 1D HC-BH model with a chemical potential μ has three phases: two Mott insulator phases, for $\mu < -1$ with $\langle n_i \rangle = 1$ and for $\mu > 1$ with $\langle n_i \rangle = 0$, separated by a gapless superfluid phase for $|\mu| < 1$. Therefore, there are two Mott insulator to superfluid transitions at $\mu = -1$ and $\mu = 1$. These transitions are characterized by the dynamic exponent $z = 2$ and the RG dimension of the chemical potential $y_\mu = 2$ [21]. The gapless superfluid phase is instead described by a free massless bosonic field theory with dynamic exponent $z = 1$, see, e.g., Ref. [23].

In 1D particle systems, the *thermodynamic* limit at fixed μ corresponds to $N, l \rightarrow \infty$ keeping the ratio N/l fixed. Indeed, we have

$$N \equiv \langle \sum_i b_i^\dagger b_i \rangle = \tilde{\rho}(\mu)l + O(1) \quad (24)$$

The function $\tilde{\rho}(\mu)$ can be computed in the HC limit. The particle density in the large- l limit turns out to approach its local density approximation (LDA), with corrections that are suppressed by powers of the trap size and present a nontrivial TSS behaviour [55]. Within the LDA, the particle density at the spatial coordinate x equals the particle density of the homogeneous system at the effective chemical potential

$$\mu_{\text{eff}}(x) \equiv \mu + \frac{1}{p} \left(\frac{x}{l} \right)^p. \quad (25)$$

The LDA of the particle density reads $\langle n_x \rangle_{\text{lda}} \equiv \rho_{\text{lda}}(x/l)$, where

$$\rho_{\text{lda}}(x/l) = \begin{cases} 0 & \text{for } \mu_{\text{eff}}(x) > 1, \\ (1/\pi) \arccos \mu_{\text{eff}}(x) & \text{for } -1 \leq \mu_{\text{eff}}(x) \leq 1, \\ 1 & \text{for } \mu_{\text{eff}}(x) < -1. \end{cases} \quad (26)$$

Asymptotically, the total particle number is obtained by integrating the LDA of the particle density ρ_{lda} , obtaining

$$\tilde{\rho}(\mu) = 2 \int_0^\infty \rho_{\text{lda}}(y) dy. \quad (27)$$

In the low-density regime, $\bar{\mu} \equiv \mu - 1 \rightarrow 0$,

$$\tilde{\rho}(\mu) = c |\bar{\mu}|^{(2+p)/(2p)} [1 + O(\bar{\mu})], \quad (28)$$

where c is a p -dependent constant; $c = 1$ for $p = 2$.

Eq. (24) provides the correspondence between the ratio N/l and μ . In particular, when $0 < N/l < \tilde{\rho}(-1)$ the system is effectively in the superfluid phase, while for $N/l > \tilde{\rho}(-1)$ the $n = 1$ Mott phase appears around the center of the trap. Eq. (27) gives $\tilde{\rho}(-1) = 2.54648$ for $p = 2$ and $\tilde{\rho}(-1) = 2.56561$ for $p = 4$. Eqs. (24), (26), and (28) imply that the particle density at the origin scales as a nontrivial power law of the ratio N/l in the low-density regime,

$$\rho(0) \sim (N/l)^\theta. \quad (29)$$

At the low-density Mott transition, around $\mu = 1$, the TSS limit can be analytically derived within the quadratic spinless fermion representation [55]. This is obtained by rescaling the spatial distance from the origin as

$$x = l^\theta X, \quad (30)$$

and the difference $\bar{\mu} \equiv 1 - \mu$ as

$$\bar{\mu} = l^{-2\theta} \mu_r. \quad (31)$$

Any low-energy scale turns out to behave as $E \approx l^{-2\theta} \mathcal{E}_\Delta(\mu_r)$, the particle density behaves as $\langle n_x \rangle \approx l^{-\theta} \mathcal{D}(\mu_r, X)$, etc..., in agreement with the scaling Ansatz reported in the previous section, cf. Eq. (12). Analytic

and numerical calculations of the above scaling functions are reported in Ref. [55].²

B. TSS of a system of N particles

We now derive the TSS as a function of the particle number N in the low density regime $Na/l \ll 1$. This is worth being discussed in some detail, because the corresponding TSS functions are not trivially derived from the TSS in the presence of a chemical potential, which were already computed in Ref. [55].

1. TSS limit

In the fermion representation the Hamiltonian

$$H_c = \sum_{ij} c_i^\dagger h_{ij} c_j \quad (32)$$

can be diagonalized by introducing new canonical fermionic variables $\eta_k = \sum_i \phi_{ki} c_i$, where ϕ satisfies the equation

$$h_{ij} \phi_{kj} = \omega_k \phi_{ki}, \quad (33)$$

so that

$$H_c = \sum_k \omega_k \eta_k^\dagger \eta_k. \quad (34)$$

The ground state of a system of N particles is then given by the η -fermions filling the N lowest one-particle levels. For the lowest states, assuming smoothness, we may consider the continuum limit of Eq. (33), by replacing $\phi_{kx} \rightarrow \phi_k(x)$ and rewriting the discrete differences as

$$\phi(x+a) - \phi(x) = a \frac{d\phi(x)}{dx} + \frac{1}{2} a^2 \frac{d^2\phi(x)}{dx^2} + \dots, \quad (35)$$

where a is the lattice spacing. Then, rewriting the resulting equation in terms of the rescaled quantities

$$X \equiv a^{-2\theta/p} l^{-\theta} x, \quad (36)$$

$$e_k \equiv a^{-2\theta} l^{2\theta} \omega_k, \quad (37)$$

$$\varphi_k(X) \equiv a^{\theta/p} l^{\theta/2} \phi_k(a^{-2\theta/p} l^\theta X), \quad (38)$$

with θ given by Eq. (10), and neglecting terms which are suppressed by powers of the trap size, one arrives at a Schrödinger-like equation

$$\left(-\frac{1}{2} \frac{d^2}{dX^2} + \frac{1}{p} X^p \right) \varphi_k(X) = e_k \varphi_k(X). \quad (39)$$

² Note that here the definition of the trap size, cf. Eq. (2), differs from that of Refs. [25, 55] by a factor $p^{-1/p}$.

This equation describes the TSS limit at fixed N , i.e., $l \rightarrow \infty, x \rightarrow \infty$, keeping the scaling variable X fixed. The next-to-leading terms in the large- l limit, arising from the higher order terms in the expansion (35), give rise to $O(l^{-2\theta})$ scaling corrections [55]. Moreover, one can easily check that a shift of the center of the trap, by $\delta < a$, generally induces $O(l^{-\theta})$ subleading corrections.

Solving Eq. (39) for $p = 2$, we obtain

$$e_k = k + 1/2, \quad k \geq 0, \quad (40)$$

$$\varphi_k(X) = \frac{H_k(X)}{\pi^{1/4} 2^{k/2} (k!)^{1/2}} \exp(-X^2/2),$$

where $X \equiv x/(al)^{1/2}$ and H_k are Hermite's polynomials. For $p = 4$, Eq. (39) can be solved numerically by Numerov's method, see, e.g., Ref. [60]; the resulting energy levels are $e_0 = 0.420805$, $e_1 = 1.50790$, $e_2 = 2.95880$, $e_3 = 4.62122$, $e_4 = 6.45350$, $e_5 = 8.42843$, etc.... The Bohr-Sommerfeld quantization formula, see, e.g., Ref. [61], gives the asymptotic large- k behavior

$$e_k \approx b_4(k + 1/2)^{4/3},$$

$$b_4 = \frac{\pi^{2/3} \Gamma(7/4)^{4/3}}{2^{4/3} \Gamma(5/4)^{4/3}} \cong 0.867145. \quad (41)$$

This formula provides a good approximation for relatively low levels already: it is accurate to 0.1% already for e_5 . For $p \rightarrow \infty$, Eq. (39) becomes equivalent to the Schrödinger equation of a free particle in a box of size $L = 2l$ with boundary conditions $\varphi(-1) = \varphi(1) = 0$, leading to

$$e_k = \frac{\pi^2}{8}(k + 1)^2, \quad k \geq 0, \quad (42)$$

$$\varphi_k(X) = \sin \left[\frac{\pi}{2}(k + 1)(X + 1) \right],$$

where $X \equiv x/l$.

In App. A we show that the same TSS limit is obtained when the trap is induced by a spatial dependence of the hopping parameter.

2. TSS of observables

In the following we set the lattice spacing $a = 1$ to simplify the expressions. The dependence on a and J can be easily recovered by a dimensional analysis.

The TSS limit leading to Eq. (39) allows us to compute the low-density trap-size dependence of the observables. For example, the gap, i.e., the difference of the energy of the lowest states, behaves as

$$\Delta_N = A_N l^{-2\theta} [1 + O(l^{-2\theta})], \quad (43)$$

with $A_2 = 1$ for $p = 2$, and

$$A_N = a_p N^{2\theta-1} [1 + O(1/N)] \quad (44)$$

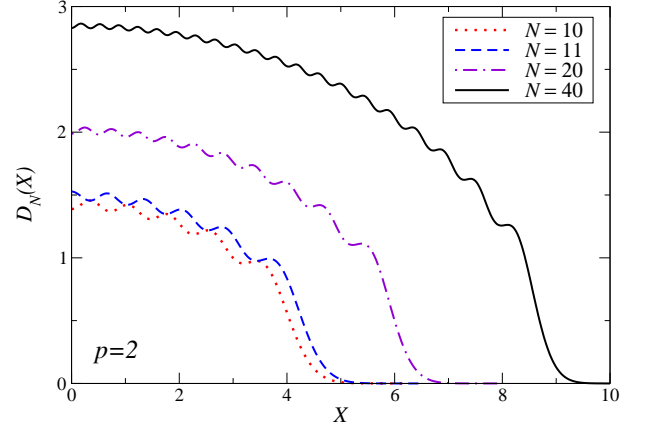


FIG. 1: (Color online) The scaling function $\mathcal{D}_N(X)$, cf. Eq. (46), for $p = 2$. Since $\mathcal{D}_N(X) = \mathcal{D}_N(-X)$ due to the reflection symmetry with respect to the center of the trap, we show only the curves for $X \geq 0$.

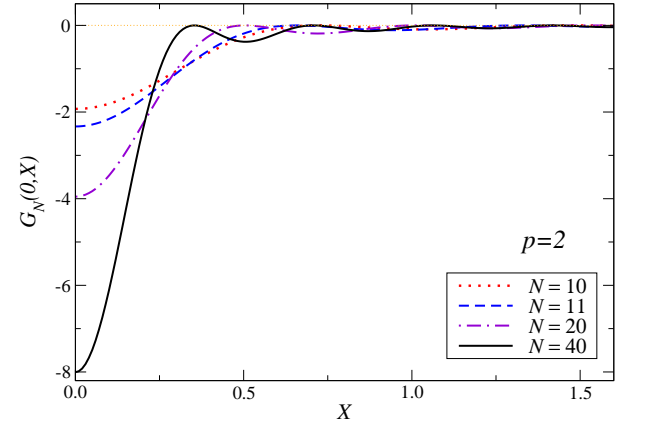


FIG. 2: (Color online) The scaling function $\mathcal{G}_N(0, X)$, cf. Eq. (48), for $p = 2$.

for a generic power law p : $a_4 \approx 1.15619$ and $a_\infty = \pi^2/2$. Note that the gap at fixed N differs from the difference of the energy of the lowest states at fixed chemical potential μ , which behaves as $\Delta_\mu = l^{-2\theta} \mathcal{E}_\Delta(\mu_r)$, because the latter involves states of subsequent particle number sectors, giving rise to zeroes in the scaling function $\mathcal{E}_\Delta(\mu_r)$ for $\mu_r < 0$, see Ref. [55].

In the low-density regime the particle density behaves as

$$\rho(x) \equiv \langle n_x \rangle = l^{-\theta} \mathcal{D}_N(X) [1 + O(l^{-2\theta})], \quad (45)$$

$$\mathcal{D}_N(X) = \sum_{k=0}^{N-1} \varphi_k^2(X). \quad (46)$$

Fig. 1 shows results for the spatial dependence of $\mathcal{D}_N(X)$ for $p = 2$ and several values of N . Note the peculiar structure of $\mathcal{D}_N(X)$ characterized by N local maxima, which get suppressed at large N by powers of $1/N$. Due to the parity of the Hermite polynomials, $\mathcal{D}_{2j-1}(0) = \mathcal{D}_{2j}(0)$.

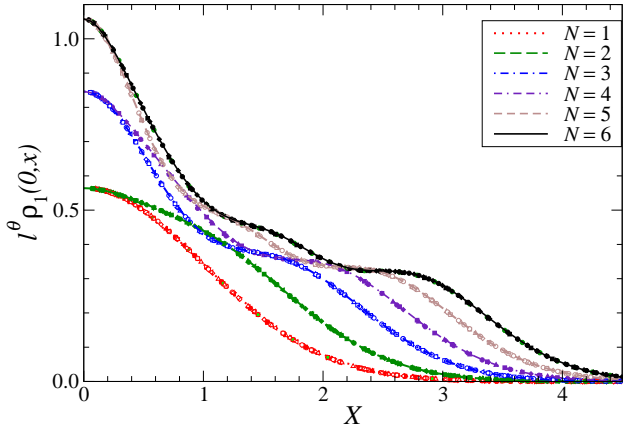


FIG. 3: (Color online) Results for the one-particle density matrix: we plot $l^\theta \rho_1(0, x)$ vs $X \equiv x/l^\theta$ for $p = 2$, thus $\theta = 1/2$, for several values of N . The data points are numerical results for the HC-BH model at fixed N and trap size l , with $10 \lesssim l \lesssim 10^3$. The continuous lines are the curves for systems of N impenetrable bosons. The data of the HC-BH model clearly approach these curves in the large trap-size limit.

Straightforward calculations show that the density-density correlator behaves as

$$G_n(x, y) \equiv \langle n_x n_y \rangle_c \approx l^{-2\theta} \mathcal{G}_N(X, Y), \quad (47)$$

where $X = x/l^\theta$, $Y = y/l^\theta$, and

$$\mathcal{G}_N(X, Y) = - \left[\sum_{k=0}^{N-1} \varphi_k(X) \varphi_k(Y) \right]^2. \quad (48)$$

Fig. 2 shows plots of $\mathcal{G}_N(0, X)$ for the harmonic potential.

The one-particle density matrix, cf. Eq. (18), cannot be easily derived from the solutions of Eq. (39), because the fermion-boson map exploited in the HC limit is not trivial, and, in particular, it is non local. However, as we shall show in Sec. IV, the asymptotic TSS of the BH model in the low-density regime coincides with the trap-size dependence of a 1D gas of impenetrable bosons, whose one-particle density matrix can be computed using the known ground-state wave function. Some results for the harmonic potential are shown in Fig. 3.

The TSS functions of the observables considered above show nontrivial power-law scalings with respect to the particle number N at large N . Their large- N behaviors are reported in App. B.

C. Numerical results

Beside deriving the asymptotic behaviors in the low-density region, we present numerical calculations at fixed particle number N and trap size l . We exploit the quadratic spinless fermion representation (22) of the 1D HC-BH model, which allows us to perform computations for very large systems, since they only require the diagonalization of a $L \times L$ matrix where L is the number

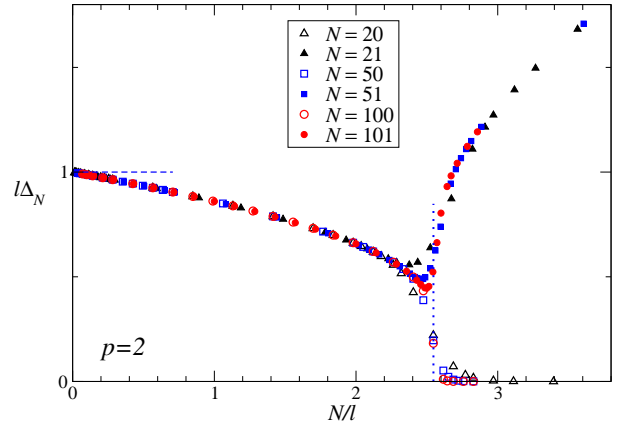


FIG. 4: (Color online) $l\Delta_N$ versus N/l for $p = 2$. The dashed horizontal line indicates the constant value computed in the low-density regime, i.e., $N/l \ll 1$. The vertical dotted line shows the asymptotic value of the ratio N/l corresponding to the $n = 1$ Mott transition.

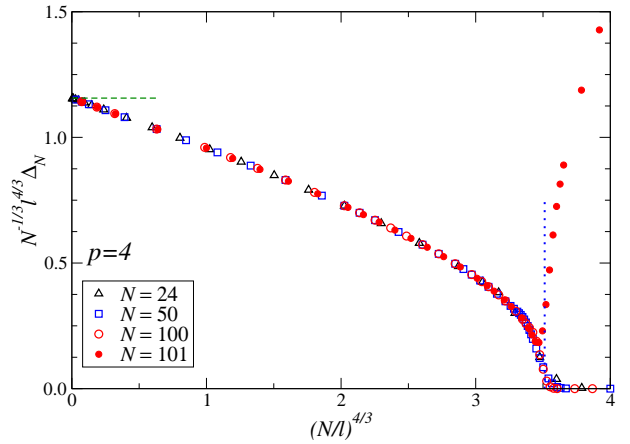


FIG. 5: (Color online) Plot of $N^{-1/3} l^{4/3} l\Delta_N$ versus $(N/l)^{4/3}$ for $p = 4$. The dashed horizontal line indicates the constant value computed in the low-density regime, i.e., $N/l \ll 1$. The vertical dotted line shows the asymptotic value of $(N/l)^{4/3}$ corresponding to the $n = 1$ Mott transition.

of lattice sites. We obtain numerical results for chains of size L , with a trap of size l centered at the middle site (we consider odd L); we choose L large enough to have negligible finite- L effects. This can be accurately checked by comparing results at fixed l and increasing values of L . Thus, the results at fixed N and l that we shall present, respectively up to $N \approx 10^2$ and $l = O(10^3)$, are the infinite chain size limit (keeping N and l fixed) with great accuracy. For more details see Ref. [55], where analogous calculations at fixed chemical potential were presented.

Bosonic particle systems confined to 1D lattices have already been the subject of several numerical investigations [24, 37, 46–48, 53, 54]. We study the dependence of some physically interesting observables on the particle number N and the trap size l .

Figs. 4 and 5 show results of the gap for $p = 2$ and

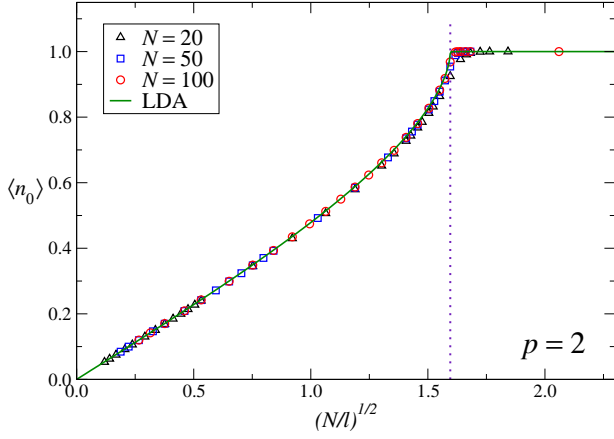


FIG. 6: (Color online) The particle density at the origin versus $(N/l)^{1/2}$, for $p = 2$ for several values of N and l . The data points show results obtained by solving the HC-BH model at fixed N and l , while the continuous line shows the LDA. The vertical dotted line shows the asymptotic value of $(N/l)^{1/2}$ corresponding to the $n = 1$ Mott transition.

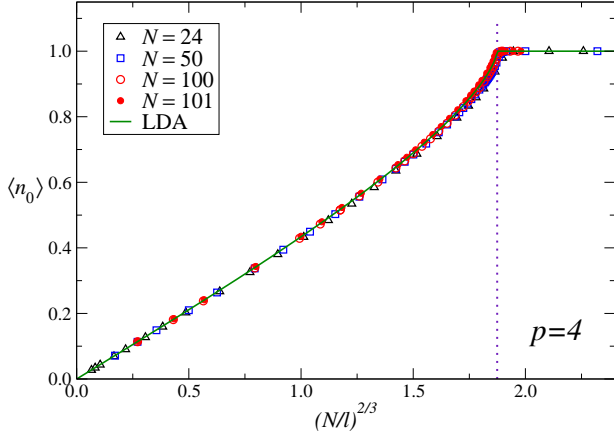


FIG. 7: (Color online) The particle density at the origin versus $(N/l)^{2/3}$, for $p = 4$. The data points show results obtained by solving the HC-BH model at fixed N and l , while the continuous line shows the LDA. The vertical dotted line shows the asymptotic value of $(N/l)^{2/3}$ corresponding to the $n = 1$ Mott transition.

$p = 4$ respectively. Note that the gap of a system of N impenetrable bosons is identical to the gap of N free fermion particles in a trap. Guided by the low-density scaling behavior (43), we plot the quantity $N^{1-2\theta}l^{2\theta}\Delta_N$ versus $(N/l)^{2\theta}$ (which is just $l\Delta_N$ vs. N/l for $p = 2$).

In the region of values of N/l corresponding to $1 > \mu > -1$, the data show the asymptotic behavior

$$N\Delta_N = g(N/l), \quad (49)$$

in the limit $l \rightarrow \infty$, $N \rightarrow \infty$ keeping N/l fixed. The low-density behavior (43) is recovered for $N/l \ll 1$, because

$$g(x) = cx^{2\theta} [1 + O(x^{2\theta})]. \quad (50)$$

Around $N/l = \tilde{\rho}(-1)$, i.e., the value corresponding to the $n = 1$ Mott transition, the behavior for even and odd N begins differing significantly. In particular, the data for even N appear suppressed for $N/l \gtrsim \tilde{\rho}(-1)$. This is essentially related to the fact that the trap is centered at the middle site of the chain. When the region around the center of the trap shows the $n = 1$ Mott phase, we have two degenerate lowest states for even N , differing for a reflection with respect to the middle site; while for odd N the ground state is unique, and the gap is expected to behave as $\Delta_N \sim N^{p-1}/l^p$ for N/l sufficiently larger than $\tilde{\rho}(-1)$, as also shown by Fig. 4 for $p = 2$, where the corresponding asymptotic behavior $l\Delta_N \sim N/l$ can be already seen for $N/l \gtrsim 3$.

Figs. 6 and 7 show results of the particle density at the origin, for $p = 2$ and $p = 4$ respectively, for some values of N in the range $20 \lesssim N \lesssim 100$, and l up to $O(10^3)$. The data appear to follow a unique function of $\tilde{\rho} \equiv N/l$, given by the LDA obtained using Eqs. (26) and (27), and corrections are hardly visible. This fact was already observed by other numerical works, see, e.g., Refs. [53, 54]. The agreement is already good for relatively small values of N , i.e., $N \gtrsim 20$. Note that the LDA reproduces the low-density behavior (45) for $N \gg 1$, and in particular the leading large- N term of Eq. (B1).

Figures 8 and 9 show results for the momentum distribution n_k , cf. Eq. (19), for $p = 2$ and $p = 4$ respectively, and several values of N and l . We first note that the plots of n_k vs k show the scaling behavior

$$n_k \approx f(N/l, k) \quad (51)$$

Moreover, as shown by the plots of $l^{-\theta}n_k$ versus $K \equiv l^\theta k$, the data also support the TSS behavior (20), which is expected to be approached with $O[(N/l)^{2\theta}]$ corrections. Actually, as shown by the bottom figures (8) and (9), the data for $k > 0$ appear to scale as

$$n_k = (N/l)^{-\theta} F(\tilde{K}), \quad \tilde{K} \equiv (N/l)^{-\theta} k, \quad (52)$$

for $N/l \ll 1$, which agrees with both Eq. (51) and (20). The zero component

$$n_0 = \frac{1}{N} \sum_{x,y} \rho_1(x, y) \quad (53)$$

scales differently, indeed $n_0 = O(1)$ in the large- N limit, analogously to a gas of impenetrable bosons. See, e.g., Ref. [42]. At large \tilde{K} , $F(\tilde{K}) \sim \tilde{K}^{-4}$, which can be inferred from the results of Refs. [62, 63] for a gas of impenetrable bosons.

D. Finite U and universality of the low-density behavior

We now consider the BH model at finite values of the on-site repulsion coupling U . We perform calculations using the DMRG method. Specifically, we consider the

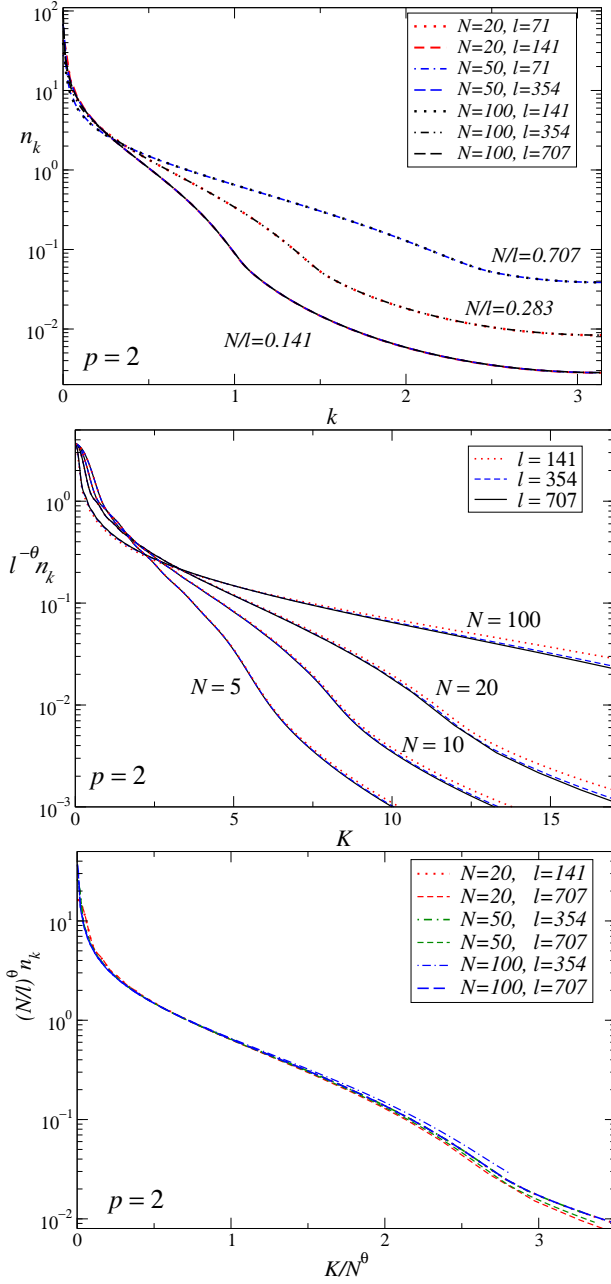


FIG. 8: (Color online) Results for the momentum distribution n_k for $p = 2$, and several values of N and l . We plot n_k vs k (above), $l^{-\theta} n_k$ versus $K \equiv l^{\theta} k$ (middle), and $(N/l)^{\theta} n_k$ vs $(N/l)^{-\theta} k$ (below). We recall that $\theta = 1/2$ for $p = 2$.

BH model with $U = 2$ in the presence of a harmonic potential, up to trap sizes $l = O(10^3)$, and for several values of N , up to $N = 20$. The trap is again centered in the middle site of a lattice of size L , which is taken sufficiently large to make finite- L effects negligible. We set the cutoff on the number of bosonic states per site $n_B = 5$, which turns out to be sufficient to provide very accurate results; indeed the relative difference from the results using $n_B = 4$ is at most $O(10^{-7})$. We keep the maximum eigenvalue truncated from the density matrix

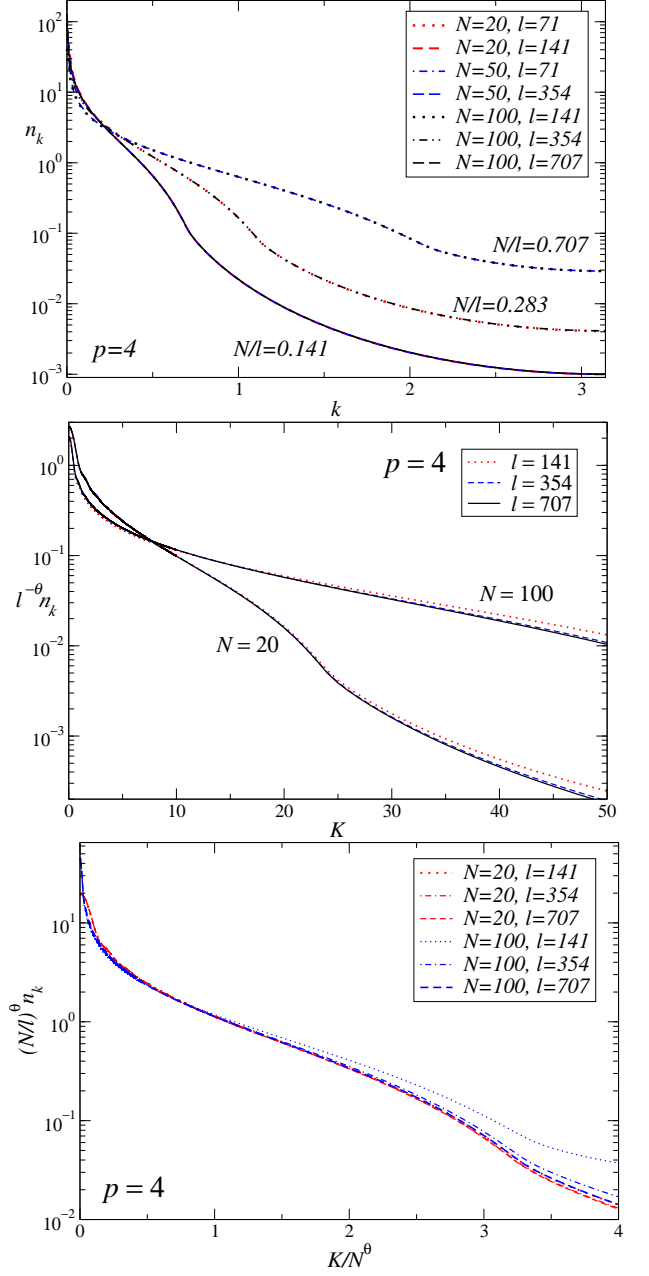


FIG. 9: (Color online) Results for the momentum distribution n_k for $p = 4$, and several values of N and l . We plot n_k vs k (above), $l^{-\theta} n_k$ versus $K \equiv l^{\theta} k$ (middle), and $(N/l)^{\theta} n_k$ vs $k/(N/l)^{\theta}$ (below). We recall that $\theta = 2/3$ for $p = 4$.

below 10^{-10} ; this requires retaining up to 200 states.

The issue that we want to investigate is the universality of the low-density TSS behavior with respect to variations of the on-site repulsion coupling U , i.e., how it depends on U . If there is universality, then the low-density asymptotic TSS at finite values of U must be the same as that found in the HC limit. Actually, a rescaling of the trap size which depends on U may be allowed, although the data show that this is not necessary when one uses the same definition of trap size with respect to

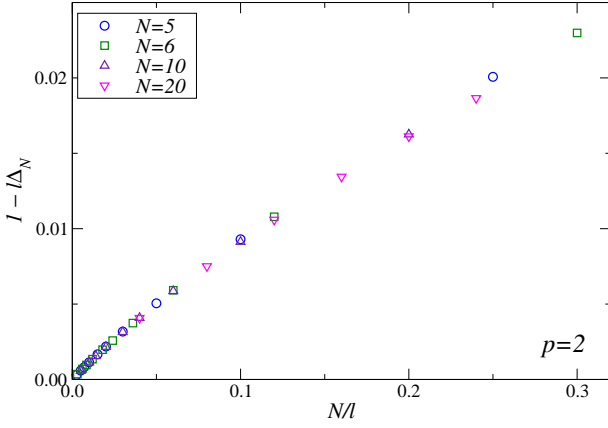


FIG. 10: (Color online) Some results for the gap of the BH model with $U = 2$ and $N = 5, 6, 10, 20$. They show that the data approach the asymptotic value $l\Delta_N = 1$ with increasing l , with $O(l^{-1})$ corrections.

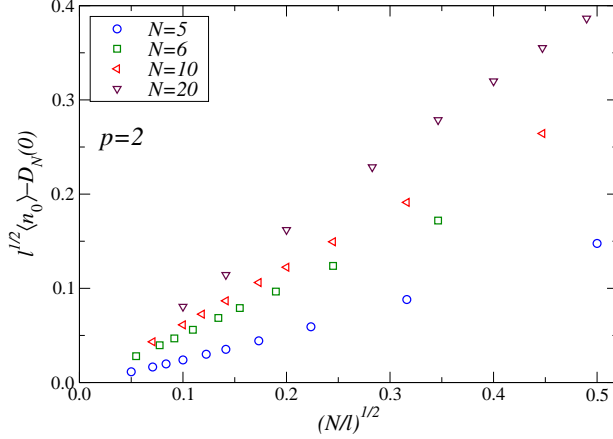


FIG. 11: (Color online) The difference $l^{1/2}\langle n_0 \rangle - \mathcal{D}_N(0)$ vs $(N/l)^{1/2}$, for the BH model with $U = 2$ and $N = 5, 6, 10, 20$. These results provide a clear evidence that the asymptotic value is consistent with $\mathcal{D}_N(0)$, and it is approached with $O(l^{-1/2})$ corrections.

the kinetic term, as we have done in Eqs. (1) and (2).

Fig. 10 shows results for the gap, i.e., the difference between the energy of the lowest states. The data show a behavior analogous to that found analytically in the HC limit, see Sec. III B 2, i.e., $l\Delta_N = 1 + O(l^{-1})$ independently of the particle number N [the large- l extrapolation to get the leading behavior is checked within an accuracy of $O(10^{-6})$]. This shows that there is no need of a U -dependent normalization of the trap size.

Fig. 11 shows data for the particle density at the origin. They are consistent with

$$l^{1/2}\rho(0) = \mathcal{D}_N(0) \left[1 + O(l^{-1/2}) \right], \quad (54)$$

where $\mathcal{D}_N(0) = \sqrt{2N}/\pi$, using Eqs. (46) and (40). Note that the power law of the scaling corrections differs from that found in the HC limit, which was $O(l^{-2\theta})$, thus

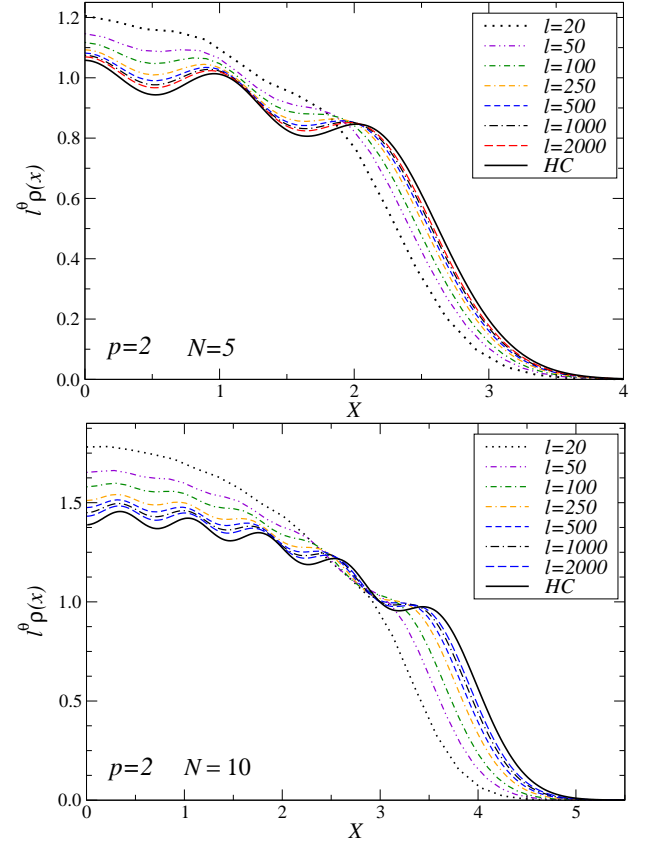


FIG. 12: (Color online) Some results for the spatial dependence of the particle density in the BH model with $U = 2$ and for $N = 5$ (above) and $N = 10$ (below). They clearly approach the large- l limit of the HC model, although their convergence appears significantly slower than that found in the HC limit.

$O(l^{-1})$ for $p = 2$. Therefore the approach to the asymptotic behavior is significantly slower than that for the HC limit. This is also found for other observables. Results for the spatial dependence of the particle density are shown in Fig. 12 for $N = 5$ and $N = 10$. They clearly approach the scaling function $\mathcal{D}_N(X)$ with increasing the trap size. Finally, in Fig. 13 we show results for the momentum distribution at several values of N , and compare them with the asymptotic behavior computed in the HC limit.

In conclusion, these results confirm that the low-density TSS of N particles described by the BH model is universal with respect to the on-site repulsion coupling U . However, scaling corrections at finite U appear generally larger than those of the HC limit, $O(l^{-\theta})$ for generic values of U against $O(l^{-2\theta})$ in the $U \rightarrow \infty$ HC limit. The only exception was the gap where we have not found evidence of $O(l^{-1/2})$ corrections.

Actually, $O(l^{-\theta})$ corrections are generally expected, because the RG dimension of the parameter U has RG dimension $y_U = -1$ with respect to the low-density scaling. This implies that it generally leads to $O(\xi^{-1})$ scaling corrections, which become $O(l^{-\theta})$ in terms of the trap

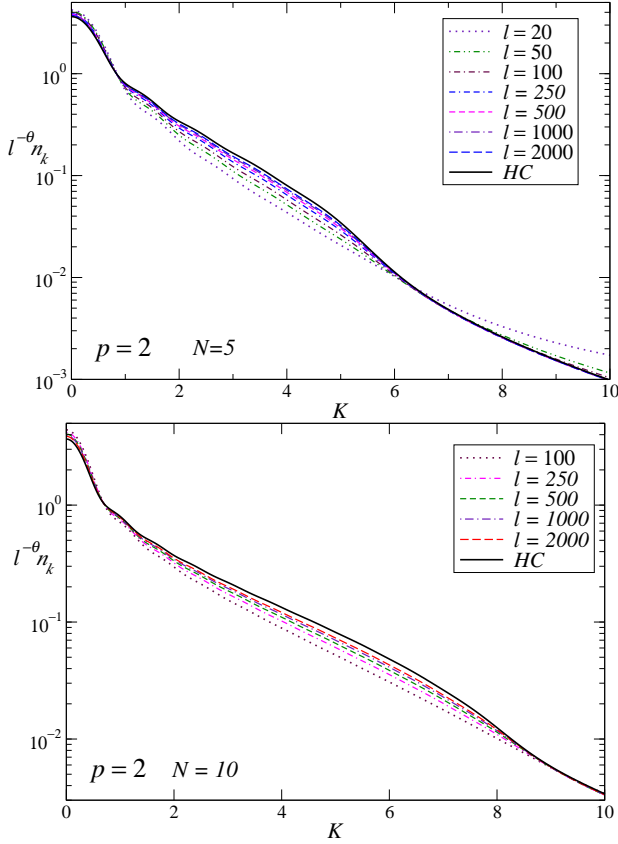


FIG. 13: (Color online) Some results for the BH model with $U = 2$ for $N = 5$ (above) and $N = 10$ (below).

size.³ These corrections vanish in the HC limit. Thus, within generic 1D BH models, the HC limit represents a RG-improved model [64] where the leading scaling corrections are absent.

IV. THE 1D BOSONIC GAS AT LOW DENSITY

We now consider a system of 1D boson particles interacting through a repulsive contact term in the presence of a confining potential such as (2), described by the LL model, cf. Eq. (4). In the low-density regime the system can be effectively described by the limit of infinitely strong repulsive interaction [30], i.e., a 1D gas of impenetrable bosons (TG model).

The wave function for a 1D system of N impenetrable bosons in a confining potential is essentially defined by

the one-particle Hamiltonian

$$H = \frac{p^2}{2m} + \frac{1}{p} m \omega^p x^p \quad (55)$$

and the impenetrability condition, i.e., the fact that the wave function of the N particles vanishes if two spatial variables coincide. The low-density condition to realize a 1D TG gas of impenetrable bosons is [2, 30] $N a_s^2 / l_{\text{osc}}^2 \ll 1$ where a_s is the 1D scattering length, related to the quartic coupling by $g = -4\hbar^2 / (m^2 a_s)$, and $l_{\text{osc}} \equiv \hbar^{1/2} / (m\omega)^{1/2}$ is the oscillator length. In the following we set $\hbar = 1$ and $m = 1$.

The ground-state wave function of the TG model can be written in terms of the ground state wave function of N free fermion particles [28, 29] described by the Hamiltonian (55), which is

$$\Psi(x_1, \dots, x_N) = \frac{1}{\sqrt{N!}} \det[\phi_i(x_j)], \quad (56)$$

where $\phi_i(x)$ are the lowest N eigensolutions of the one-particle Schrödinger equation $H\phi_i = E_i\phi_i$. The wave function Φ of N impenetrable bosons is obtained by *symmetrizing* the fermion wave function Ψ , i.e.,

$$\Phi(x_1, \dots, x_N) = \mathcal{A}(x_1, \dots, x_N) \Psi(x_1, \dots, x_N), \quad (57)$$

$$\mathcal{A}(x_1, \dots, x_N) = \prod_{1 \leq i < j \leq N} \text{sign}(x_i - x_j). \quad (58)$$

The ground-state wave function allows us to derive the one- and two-particle density matrices by

$$\rho_1(x, y) = N \int \Phi(x, x_2, \dots, x_N)^* \Phi(y, x_2, \dots, x_N) dx_2 \dots dx_N \quad (59)$$

and

$$\begin{aligned} \rho_2(x_1, x_2; y_1, y_2) = & \quad (60) \\ N^2 \int \Phi(x_1, x_2, x_3, \dots, x_N)^* \Phi(y_1, y_2, x_3, \dots, x_N) dx_3 \dots dx_N. \end{aligned}$$

In the case of the harmonic potential, we have

$$\begin{aligned} E_k &= \omega(k + 1/2), \quad k \geq 0, \\ \phi_k(x) &= \omega^{1/4} \frac{H_k(\omega^{1/2} x)}{\pi^{1/4} 2^{k/2} (k!)^{1/2}} e^{-\omega x^2/2}, \end{aligned} \quad (61)$$

thus leading to [35]

$$\begin{aligned} \Phi(x_1, \dots, x_N) &= c_N \omega^{N^2/4} B(x_1, \dots, x_N) e^{-\sum_i \omega x_i^2/2}, \\ B(x_1, \dots, x_N) &= \prod_{1 \leq i < j \leq N} |x_i - x_j|, \end{aligned} \quad (62)$$

where c_N is the appropriate normalization constant

$$c_N = \pi^{-N/4} \left[N! \prod_{k=0}^{N-1} 2^{-k} k! \right]^{-1/2}, \quad (63)$$

³ The RG dimension of U can be derived from the β -function associated with the quartic term of the corresponding bosonic continuum theory (9), which reads $\beta(u) = u - u^2/2$ exactly [23]. It has a nontrivial fixed point for $u^* = 2$, thus $y_U = \beta'(u^*) = -1$.

so that $\int \prod_{i=1}^N dx_i |\Phi|^2 = 1$. Some useful analytical developments, to evaluate the one-particle density matrix, can be found in Refs. [36, 40, 42, 43, 45, 50].

We now note that, after appropriate rescalings, the above results for the TG model coincide with the low-density TSS of the BH model, see Sec. III B 1, which was derived by taking the continuum TSS limit of its HC limit. This implies that the trap-size dependence of the TG model exactly gives the asymptotic TSS of BH model, after replacing $^4 l = \omega^{-1}$. This can be verified by explicit calculations, see below.

Straightforward calculations lead to the following expressions for the particle density and its correlator:

$$\rho(x) \equiv \rho_1(x, x) = l^{-\theta} \mathcal{D}_N(X) \quad (65)$$

and

$$\begin{aligned} G_n(x, y) &= \langle n_x n_y \rangle_c = \\ &= \rho_2(x, y; x, y) - \rho_1(x, x) \rho_1(y, y) \\ &= l^{-2\theta} \mathcal{G}_N(X, Y) \end{aligned} \quad (66)$$

where $\theta = p/(p+2)$ is the trap exponent already introduced in the low-density TSS of the BH model, $X = x/l^\theta$ and $Y = y/l^\theta$, and the TSS functions \mathcal{D}_N and \mathcal{G}_N are exactly given by Eqs. (46) and (48).

The one-particle density matrix can be written as

$$\rho_1(x, y) = l^{-\theta} \mathcal{M}_N(X, Y). \quad (67)$$

Again, this exactly provides the large- l TSS of the BH model, as shown by results for the TG model and the HC-BH model in Fig. 3. In particular, its large- N limit is given by Eq. (B6), which implies that the rescaled density matrix $(N/l)^{-\theta} \rho_1(x, y)$ has a nontrivial large- N limit $B(\zeta, \delta)$ keeping $\zeta \equiv xN^{-1+\theta}l^{-\theta}$ and $\delta \equiv (y-x)N^{-\theta}l^{-\theta}$ fixed. This scaling behavior was already noted in Ref. [42].

We can also compute the energy difference Δ_N between the two lowest states. The lowest excited state above the ground state is obtained by *exciting* only the *fermion* particle with the highest energy in the ground state. One can easily check that Δ_N is exactly given by the asymptotic TSS behavior found for the HC-BH model, cf. Eq. (43), without corrections. In particular, $\Delta_N = 1/l$ for the harmonic potential.

⁴ Restoring the dependences on J, a and m in the BH and TG models, the trap-size correspondence between the *trap sizes* of the BH and TG models is

$$a^{2/p} l = \frac{a^{2/p} J^{1/p}}{v} \leftrightarrow \frac{\hbar^2/p}{m^{2/p} \omega}, \quad (64)$$

thus $l = \omega^{-1}$ setting J, a, m to one. Therefore, the trap size of the TG model in a harmonic potential is essentially given by $l \sim \hbar/(m\omega)$, thus $l \sim l_{\text{osc}}^2$ where $l_{\text{osc}} \equiv \sqrt{\hbar/(m\omega)}$ is the characteristic length scale of an oscillator of frequency ω .

Summarizing, we have shown that the trap-size dependence in a 1D trapped gas of N impenetrable bosons coincides with the asymptotic TSS of N particles described by the 1D BH model, if appropriate definitions of the trap size are considered. As already argued within the BH model, the critical exponents associated with this TSS are related to the *nonrelativistic* Φ^4 theory (9). We expect that the low-density TSS is also universal with respect to the strength of the short-ranged repulsive interaction. Therefore, it should exactly provide the asymptotic low-density trap-size dependence of N boson particles described by the LL model, when $Na_s^2/l_{\text{osc}}^2 \ll 1$.

Note that the power-law TSS does not have corrections in trapped systems of impenetrable bosons, while within the BH model it is only expected asymptotically in the large- l limit, i.e., it is approached with $O(l^{-2\theta})$ corrections in the HC limit and $O(l^{-\theta})$ corrections for finite U . In a sense, in the language of the RG theory [65], the TG model represents a fixed-point Hamiltonian, i.e., a model where scaling corrections are totally absent, with respect to the low-density behavior of the BH model and the LL gas. Using the same RG arguments reported at the end of Sec. III D, we predict that scaling corrections are $O(l^{-\theta})$ in the LL model.

V. TRAP-SIZE SCALING IN A TIME-DEPENDENT TRAP

The off-equilibrium dynamics is a quite complicated issue, more subtle than issues related to the equilibrium behavior. This is not a prerogative of the quantum evolution only, but it is also found in classical systems, see, e.g., Refs. [66, 67].

In this section we discuss the trap-size dependence of the off-equilibrium time evolution of 1D bosonic gases in time-dependent traps, in the limit of instantaneous variations and for a power-law time dependence, starting from the equilibrium ground state for a initial trap size l_0 . We derive scaling Ansatz for the asymptotic TSS with respect to the initial trap size l_0 in the large- l_0 limit.

A. Instantaneous variation of the confining potential

Let us first discuss the case of an instantaneous change of the confining potential. In particular, we assume that at $t = 0$ the N -particle system is at equilibrium, in the ground state with a confining potential of trap size l_0 . Then, the trap is instantaneously changed to a larger trap size, $l_f > l_0$, or dropped completely, corresponding to $l_f = \infty$. We are interested in the asymptotic trap-size dependence of the quantum time evolution after the instantaneous quench for large initial trap size l_0 .

In this case we expect that the trap-size dependence of the off-equilibrium dynamics after the quench is essentially determined by the trap-size dependence of the

initial state at equilibrium, and by the ratio l_f/l_0 of the final and initial trap sizes. Thus, the simplest scaling Ansatz for the large- l_0 behavior may be

$$\langle O \rangle_N(x; t) \approx l_0^{-y_o \theta} \mathcal{O}_N(x l_0^{-\theta}, t l_0^{-z \theta}, l_f/l_0), \quad (68)$$

where $z = 2$ and $\theta = p/(p+2)$ is the equilibrium trap exponent. For example, this would imply that the particle density of 1D and 2D bosonic gases behaves as

$$\rho(x; t) \approx l_0^{-d \theta} \mathcal{D}_N(x l_0^{-\theta}, t l_0^{-z \theta}, l_f/l_0). \quad (69)$$

This scaling Ansatz will be confirmed by the time evolution of a 1D gas of impenetrable bosons, see Sec. VII B. We also expect that, like the equilibrium behavior, 1D impenetrable boson gases and 1D BH models of N particles share the same TSS of the off-equilibrium dynamics after instantaneous variations of the trap.

B. Power-law time dependence of the confining potential

A non trivial time dependence of the confining potential makes the issue more complicated. In the following, we consider a power-law time dependence, such as that given by Eqs. (5) and (6). We are again interested in the asymptotic trap-size dependence of the quantum time evolution for large initial trap size l_0 .

We use RG scaling arguments to infer the scaling behavior of the time dependence of generic observables under a change of the confining potential. For this purpose, we write the perturbation associated with the time-dependent confining potential to the continuum theory (9), i.e.,

$$\int d\tau d^d x u^p \tau^q |x|^p |\phi(x, \tau)|^2, \quad (70)$$

where τ indicates a time variable. We are interested in the scaling behavior at fixed N , large l_0 , with $N/l_0 \ll 1$. The RG arguments of Sec. II, see also Ref. [25], may be extended to allow for the presence of a time-dependent perturbation (70), and derive an off-equilibrium scaling Ansatz. A standard analysis of the RG dimensions of the coupling u leads to [25, 56] $y_u = (2 + p + zq)/p$. It is convenient to introduce the initial trap size at $t = 0$, $l_0 = 1/u$, with the corresponding RG dimension

$$\theta_0 = \frac{p}{2 + p + zq}. \quad (71)$$

Let us consider an operator O whose low-density critical behavior of its matrix elements is described by the RG dimension y_o in the homogeneous system. In the presence of a chemical potential, the simplest Ansatz for the large- l_0 off-equilibrium behavior, which may be derived from the above RG scaling arguments, is

$$\langle O \rangle(\mu, x; t) \approx l_0^{-y_o \theta_0} A_0(x l_0^{-\theta_0}, \tau l_0^{-z \theta_0}, \bar{\mu} l_0^{y_\mu \theta_0}). \quad (72)$$

The corresponding Ansatz for the low-density TSS at fixed particle number N is

$$\langle O \rangle_N(x; t) \approx l_0^{-y_o \theta_0} \mathcal{O}_N(x l_0^{-\theta_0}, \tau l_0^{-z \theta_0}). \quad (73)$$

For example, the application to the one-particle density matrix reads

$$\rho_1(x_1, x_2; t) \approx l_0^{-\theta_0} \mathcal{M}_N(x_1 l_0^{-\theta_0}, \tau l_0^{-z \theta_0}). \quad (74)$$

We warn that these scaling behaviors neglect possible relevant effects related to the initial conditions, which may not allow us to take the $l_0 \rightarrow \infty$ limit of the scaling functions \mathcal{O}_N , more precisely of the product $l_0^{y_o \theta_0} \langle O \rangle_N(x; t)$ after the variable rescalings $X \equiv x l_0^{-\theta_0}$ and $Z \equiv \tau l_0^{-z \theta_0}$.

The above scaling Ansatz can be reexpressed in terms of the instantaneous trap size

$$l(t) = l_0 \tau^{-q/p}. \quad (75)$$

Replacing it in Eq. (73), we can write

$$\langle O \rangle_N(x; t) \sim l(t)^{-y_o \theta} \tilde{\mathcal{O}}_N(x l(t)^{-\theta}, \tau l(t)^{-z \theta}). \quad (76)$$

The RG arguments leading to the scaling Ansatz (72) and (73) are quite general and can be applied to other models. In Ref. [56] they were applied to the XY chain in a space- and time-dependent trasverse field. In the following we challenge them against the off-equilibrium evolution of 1D bosonic particle systems.

VI. N PARTICLES IN A SLOWLY TIME-DEPENDENT TRAP

We here discuss the behavior of N particles in a time-dependent confining potential, which varies slowly, i.e., with a large parameter t_q in Eq. (5), and for sufficiently large trap sizes to be in the low-density regime. More precisely, we assume that the external potential is slowly varied so that the trap size slowly increases, corresponding to the limit $t_q \rightarrow -\infty$ in Eq. (6), thus $l(t) \rightarrow \infty$ for $t \rightarrow |t_q|$.

A. Adiabatic evolution

In the case of slow changes of the Hamiltonian parameters, the system undergoes a quasi-equilibrium dynamics, i.e., starting from the ground state at $t = 0$, the evolution of the system passes through the instantaneous ground states of the BH Hamiltonian with the confining potential $V(r, t)$ and trap size $l(t)$. We write the solution of the Schrödinger equation,

$$i \partial_t \Psi(t) = \mathcal{H}(t) \Psi(t), \quad (77)$$

in terms of the instantaneous eigenstates ϕ_n of the time-dependent Hamiltonian (whose spectrum is discrete for any finite trap size), where $\phi_n(t)$ are solutions of

$$\mathcal{H}(t)\phi_n(t) = E_n(t)\phi_n(t). \quad (78)$$

Starting at $t = 0$ from the ground state of the Hamiltonian at $t = 0$, i.e., $\Psi(0) = \phi_0(0)$, and writing

$$\Psi(t) = e^{-i\Theta_0(t)} \sum_n \alpha_n(t) \phi_n(t) \quad (79)$$

where

$$\Theta_n(t) = \int_0^t E_n(t') dt', \quad (80)$$

the zero-order adiabatic approximation gives

$$\alpha_n(t) = \delta_{n0}. \quad (81)$$

Note that the adiabatic quasi-equilibrium evolution requires the absence of degeneracies and level crossings during the process, but the *instantaneous* gap vanishes when $\tau \equiv 1 + t/t_q \rightarrow 0$. Thus we may already expect that, approaching the time corresponding to $\tau = 0$, the adiabatic condition breaks down at some point of the evolution. We return to this point later.

Under the quasi-equilibrium dynamics due to the slow increasing of the trap size, the particle number N is conserved because the particle number operator commutes with the time-dependent Hamiltonian. Since the system passes through equilibrium ground states, we can use the results obtained for the equilibrium TSS, see Secs. II, III, and IV. The adiabatic evolution of a generic observable O can be obtained by computing its expectation values over the *instantaneous* ground states. After a sufficiently large time, when $N/l(t) \ll 1$, we are in the low-density regime, thus the adiabatic time-dependence of the observables is obtained from the static low-density behaviors, such as (43) and (45), by replacing l with the instantaneous trap size (75), i.e.,

$$\langle O \rangle_{\text{adiab}}(x; t) \sim l(t)^{-y_0\theta} \mathcal{O}_N(xl(t)^{-\theta}), \quad (82)$$

where $l(t)$ is the instantaneous trap size (75). Note that this is compatible with the dynamic TSS derived in Sec. V, cf. Eqs. (76) and (73).

At large N , we may use the relation (27) to define a time-dependent chemical potential $\mu(t)$ at any t , by replacing l with $l(t)$, along the quasi-equilibrium evolution. For example in the 1D HC-BH model, since $l(t) \rightarrow \infty$ for $t \rightarrow \infty$ and therefore $N/l(t) \rightarrow 0$, we have that $\mu(t) \rightarrow 1$, which is the location of the low-density to empty-state transition. Within the adiabatic dynamics, the time behavior of the observables related to the ground state can be read from that at equilibrium, by replacing the instantaneous trap size $l(t)$ and chemical potential $\mu(t)$, obtained from Eq. (27), in the corresponding TSS formulae obtained in Ref. [55]. It is then convenient to define

$$\bar{\mu}(t) \equiv \mu(t) - 1, \quad (83)$$

which tends to zero from below in the large- t limit (after $t_q \rightarrow -\infty$). Asymptotically, when $|\bar{\mu}(t)| \ll 1$, the time dependence corresponds to varying the trap size $l(t)$ so that

$$|\bar{\mu}(t)|l(t)^{2\theta} = bN^{2\theta} \left\{ 1 + O[(N/l)^{2\theta}] \right\}, \quad (84)$$

where b is a p -dependent constant which can be easily derived from Eq. (27), for example $b = 1$ for $p = 2$. Note that the l.h.s. of Eq. (84) corresponds to the rescaled chemical potential $\mu_r \equiv l^{2\theta}\bar{\mu}$, cf. Eq. (31), and that it remains constant during the adiabatic changes since the r.h.s. remains fixed, apart from suppressed corrections.

B. First-order adiabatic perturbation theory and breaking of the adiabatic condition

We may also consider the first-order correction to Eq. (81) within the adiabatic perturbation theory, see, e.g., Refs. [68, 69]. The first-order approximation of the coefficients for $n > 0$ of the expansion (79) over instantaneous bases is

$$\alpha_n(t) \approx -e^{i\Delta\Theta_{n0}(t)} \int_0^t dt' \langle n | \partial_{t'} | 0 \rangle e^{-i\Delta\Theta_{n0}(t')}, \quad (85)$$

where $\Delta\Theta_{nm} \equiv \Theta_n - \Theta_m$, and, assuming nondegenerate states,

$$\langle n | \partial_t | 0 \rangle = -\frac{\langle n | \partial_t \mathcal{H} | 0 \rangle}{E_n(t) - E_0(t)}. \quad (86)$$

In the low-density regime, we can use the equilibrium TSS developed in the previous sections, to evaluate the first-order adiabatic approximation of the coefficients $\alpha_n(t)$. Energy differences behave as

$$E_n(t) - E_0(t) = e_n l(t)^{-z\theta}, \quad (87)$$

where e_n generally depends on the instantaneous eigenstate $|n\rangle$. The scaling behavior of the matrix element $\langle n | \partial_t \mathcal{H} | 0 \rangle$ is computed considering t as a parameter. We evaluate the matrix element between the ground state $|0\rangle$ and one of the excited states $|n\rangle$ in the low-density and TSS limit. We generally expect

$$\langle n | \partial_t \sum_i [x_i/l(t)]^p b_i^\dagger b_i | 0 \rangle = g_n \partial_t [l(t)^{-z\theta}], \quad (88)$$

where g_n is a (eigenstate-dependent) constant. Some of the lowest excited states, and in particular the lowest one, are obtained by *exciting* only the particle with the highest energy in the ground state, from the one-particle state $k = N - 1$ to $k = N - 1 + 2j$ with $j > 0$. In the case of 1D HC model we have

$$\begin{aligned} \langle e | \sum_i V(x_i) b_i^\dagger b_i | 0 \rangle &= \langle e | \sum_i V(x_i) \phi_{ki} \phi_{qi} \eta_k^\dagger \eta_q | 0 \rangle \\ &\approx l^{-z\theta} \int dX (X^p/p) \varphi_{N-1+2j}(X) \varphi_{N-1}(X), \end{aligned} \quad (89)$$

where N is the number of particles, and the functions $\varphi_k(X)$ are the solutions of Eq. (39). Thus the integral is finite. It increases as $N^{2\theta}$ at large N . In particular, for $p = 2$

$$\int dX (X^2/2) \varphi_{N+1}(X) \varphi_{N-1}(X) = \frac{N}{4} [1 + O(N^{-1})]. \quad (90)$$

The matrix element $\langle e | \partial_t \mathcal{H} | 0 \rangle$ is then obtained by performing the time derivative of the r.h.s. of Eq. (89), in agreement with Eq. (88). These results apply also to a 1D gas of impenetrable bosons.

Inserting Eq. (87) and Eq. (89) in the first-order adiabatic expansion (85) of the coefficients $\alpha_n(t)$, and defining the scaling variable $Z \equiv \tau l_0^{-z\theta_0}$, where θ_0 is the off-equilibrium trap exponent (71), we obtain

$$\alpha_n(t) \approx e^{ie_n t_q Z^{b+1}/b} \int_{Z_0}^Z \frac{d\zeta}{\zeta} \frac{bg_n}{e_n} e^{-it_q e_n \zeta^{b+1}/b} \quad (91)$$

where $b = zq\theta/p$. This expression agrees with the scaling Ansatz (72).

Note that it diverges logarithmically when $Z \rightarrow 0$,

$$\alpha_n(t) \approx \frac{bg_n}{e_n} \ln(Z/Z_0) \sim \ln[l(t)/l_0] \sim \ln \tau. \quad (92)$$

Since the adiabatic perturbative expansion requires $|\alpha_n(t)| \ll 1$, it fails when τ becomes too small. This is not unexpected because when $\tau \rightarrow 0$ the spectrum tends to be degenerate.

A simple example of the breaking of the adiabatic evolution when approaching a Hamiltonian with vanishing instantaneous gap is provided by a quantum oscillator with a time-dependent frequency, see App. C.

VII. 1D IMPENETRABLE BOSONS IN A TIME-DEPENDENT HARMONIC TRAP

In this section we determine the trap-size dependence of the off-equilibrium evolution of a 1D gas of impenetrable bosonic particles in a time-dependent confining harmonic potential, i.e., $p = 2$, starting from an equilibrium ground state configuration with initial trap size l_0 . We consider instantaneous changes to a confining potential with different trap size l_f , and also power-law time dependences such as

$$V(x, t) = \frac{1}{2} \kappa(t) x^2, \quad (93)$$

where

$$\kappa(t) = \kappa_0 \tau^q \equiv \frac{1}{l(t)^2}, \quad \tau \equiv 1 + t/t_q, \quad \kappa_0 \equiv 1/l_0^2, \quad (94)$$

and t_q is a time rate. In the following analyses of the power-law time dependence, we set $t_q = 1$ for simplicity.

A. Off-equilibrium time evolution

As shown in Ref. [31], see also [49], the time-dependent wave function of the system can be derived from the solutions $\psi_j(x, t)$ of the one-particle Schrödinger equation

$$i\partial_t \psi_j(x, t) = \left[-\frac{1}{2} \partial_x^2 + V(x, t) \right] \psi_j(x, t), \quad (95)$$

with the initial condition $\psi_j(x, 0) = \phi_j(x)$ where $\phi_j(x)$ are the eigensolutions of the Hamiltonian at $t = 0$, characterized by a trap size l_0 , with eigenvalue $E_j = (j + 1/2)/l_0$, cf. Eqs. (61). The solution can be obtained introducing a time-dependent function $s(t)$, writing [31, 70]

$$\begin{aligned} \psi_j(x, t) = & s^{-1/2} \phi_j(x/s) \times \\ & \times \exp \left(i \frac{\dot{s} x^2}{2s} - i E_j \int_0^t s^{-2} dt' \right), \end{aligned} \quad (96)$$

where $\phi_j(x)$ is the j^{th} eigenfunction of the Schrödinger equation of the one-particle Hamiltonian at $t = 0$, thus with trap size l_0 , and $s(t)$ satisfies the nonlinear differential equation

$$\ddot{s} + \kappa(t)s = \kappa_0 s^{-3} \quad (97)$$

with initial conditions $s(0) = 1$ and $\dot{s}(0) = 0$.

The time-dependent wave function Φ of N impenetrable bosons, with $\Phi(x, 0)$ given by the ground state of the Hamiltonian at $t = 0$, can be obtained following the same steps as at equilibrium, see Sec. IV, obtaining [32]

$$\begin{aligned} \Phi(x_1, \dots, x_N; t) &= \mathcal{A}(x_1, \dots, x_N) \Psi(x_1, \dots, x_N; t), \\ \Psi(x_1, \dots, x_N; t) &= \frac{1}{\sqrt{N!}} \det[\psi_i(x_j; t)], \end{aligned} \quad (98)$$

where the determinant involves the N lowest eigensolution at a fixed t . Then, using Eq. (96), one can write the wave function of the ground state of an N -particle system as

$$\begin{aligned} \Phi(x_1, \dots, x_N; t) &= s^{-N/2} \Phi(x_1/s, \dots, x_N/s; 0) \times \\ &\times \exp \left(\frac{i\dot{s}}{2s} \sum_j x_j^2 - i \sum_j E_j \int_0^t s^{-2} dt' \right), \end{aligned} \quad (99)$$

where $\Phi(x_1, \dots, x_N; 0)$ is the wave function of the ground state for the Hamiltonian at $t = 0$. The time-dependent one-particle density matrix reads [49]

$$\begin{aligned} \rho_1(x, y; t) &= \\ &= N \int \Phi(x, x_2, \dots, x_N; t)^* \Phi(y, x_2, \dots, x_N; t) dx_2 \dots dx_N \\ &= s^{-1} \rho_1(x/s, y/s; 0) \exp \left[i \frac{\dot{s}}{2s} (y^2 - x^2) \right], \end{aligned} \quad (100)$$

where $\rho_1(x, y; 0)$ is the equilibrium one-particle density matrix at a trap size $l = l_0$, i.e.,

$$\rho_1(x, y; 0) = \rho_1(x, y)|_{l=l_0}, \quad (101)$$

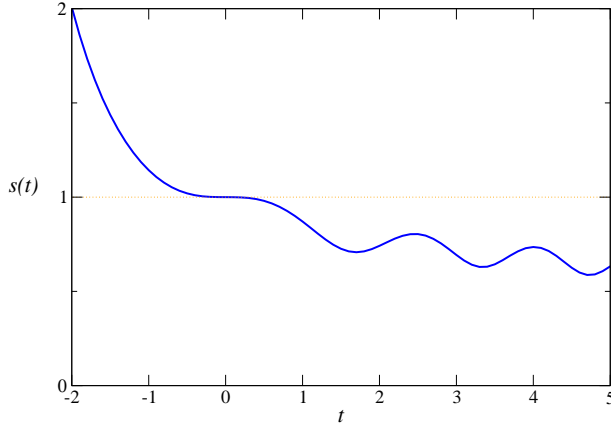


FIG. 14: (Color online) The function $s(t)$ for $\kappa_0 = 1$, cf. Eq. (104).

computed in Sec. IV, cf. Eq. (59).

Examples of explicit solutions of the function $s(t)$, cf. Eq. (97), are the following.

(i) Instantaneous drop of the trap, so that $\kappa(t) = 0$ for $t > 0$,

$$s(t) = \sqrt{1 + \kappa_0 t^2}. \quad (102)$$

(ii) Instantaneous change to a confining potential with trap size l_f , so that $\kappa(t) = l_f^{-2}$ for $t > 0$,

$$s(t) = \sqrt{1 + (r^2 - 1) \left[\sin(\kappa_0^{1/2} t/r) \right]^2}, \quad (103)$$

where $r = l_f/l_0$.

(iii) Linear time dependence of the trapping potential, i.e., $q = 1$ in Eq. (94),

$$s(t) = [\text{Re}W(\tau)]^{-1/2}, \quad \dot{s}(t) = -\frac{\kappa_0^{1/2} \text{Im}W(\tau)}{[\text{Re}W(\tau)]^{1/2}}, \quad (104)$$

where the complex function $W(\tau)$ is the solution of the differential equation

$$iW' = \kappa_0^{1/2}(W^2 - \tau) \quad (105)$$

with $W(1) = 1$,⁵ which can be written as a combination of Airy functions, [52]

$$W(\tau) = i\kappa_0^{-1/6} \frac{\text{Bi}'(-\kappa_0^{1/3}\tau) + c\text{Ai}'(-\kappa_0^{1/3}\tau)}{\text{Bi}(-\kappa_0^{1/3}\tau) + c\text{Ai}(-\kappa_0^{1/3}\tau)},$$

$$c = -\frac{\kappa_0^{1/6}\text{Bi}(-\kappa_0^{1/3}) - i\text{Bi}'(-\kappa_0^{1/3})}{\kappa_0^{1/6}\text{Ai}(-\kappa_0^{1/3}) - i\text{Ai}'(-\kappa_0^{1/3})}. \quad (106)$$

A plot of $s(t)$ is shown in Fig. 14.

⁵ In the general case, i.e., when $V(x;t) = \kappa(t)x^2/2$, the replacement (104) leads to the differential equation $iW' = \kappa_0^{1/2}W^2 - \kappa_0^{-1/2}\kappa(\tau)$ with $W(1) = 1$.

B. TSS at instantaneous quenches

We now show that the time evolution after instantaneous changes of the trap size is consistent with the scaling Ansatz put forward in Sec. V A in terms of the equilibrium trap exponent $\theta = 1/2$.

Let us first consider an instantaneous drop of the trap. The energy after the quench can be computed within 1D BH model in the TSS limit, by evaluating the expectation value of the unconfined BH Hamiltonian \mathcal{H}_u over the ground state $|0_c\rangle$ of the confined BH Hamiltonian

$$\mathcal{H}_c = \mathcal{H}_u + \sum_i V(x_i)n_i \quad (107)$$

in the low-density region $N/l \ll 1$. We have

$$E_i \equiv \langle 0_c | \mathcal{H}_u | 0_c \rangle = \langle 0_c | \mathcal{H}_c - \sum_i V(x_i)n_i | 0_c \rangle. \quad (108)$$

For $p = 2$, we have

$$E_i = l_0^{-1} \left[\sum_{k=0}^{N-1} (k + 1/2) - \int dX (X^2/2) \sum_{k=0}^{N-1} \varphi_k(X)^2 \right] = \frac{N^2}{4l_0}. \quad (109)$$

For generic values of p , we have $E_i \sim N^{2\theta+1}/l^{2\theta}$. Therefore, for large initial trap size l_0 , thus $N/l_0 \ll 1$, only low-energy states are involved.

We again expect that in the low-density regime the asymptotic trap-size dependence is that of the gas of impenetrable bosons, and that the lattice structure of the BH model gives only rise to suppressed power-law corrections. Therefore, in the case of the harmonic trap we can use the general solutions reported in the previous subsection to derive the TSS behavior at a quench.

The time-dependence of the one-particle density matrix, after turning the trap off, is obtained by inserting the function $s(t)$ of Eq. (102) into Eq. (100). Then, using equilibrium relation

$$\rho_1(x, y; 0) \approx l_0^{-\theta} \mathcal{M}(x/l_0^\theta, y/l_0^\theta), \quad (110)$$

and defining

$$X = x/l_0^\theta, \quad Y = y/l_0^\theta, \quad Z = t/l_0^{z\theta}, \quad (111)$$

$$Q(Z) = \sqrt{1 + Z^2}, \quad (112)$$

where $\theta = 1/2$ is the equilibrium trap exponent, we write

$$\rho_1(x, y; t) = l_0^{-\theta} Q^{-1} \times \times \mathcal{M}_N(X/Q, Y/Q) \exp \left[i \frac{Q'}{2Q} (Y^2 - X^2) \right]. \quad (113)$$

The particle density is given by

$$\rho(x; t) = \rho_1(x, x; t) = l_0^{-\theta} Q^{-1} \mathcal{D}_N(X/Q), \quad (114)$$

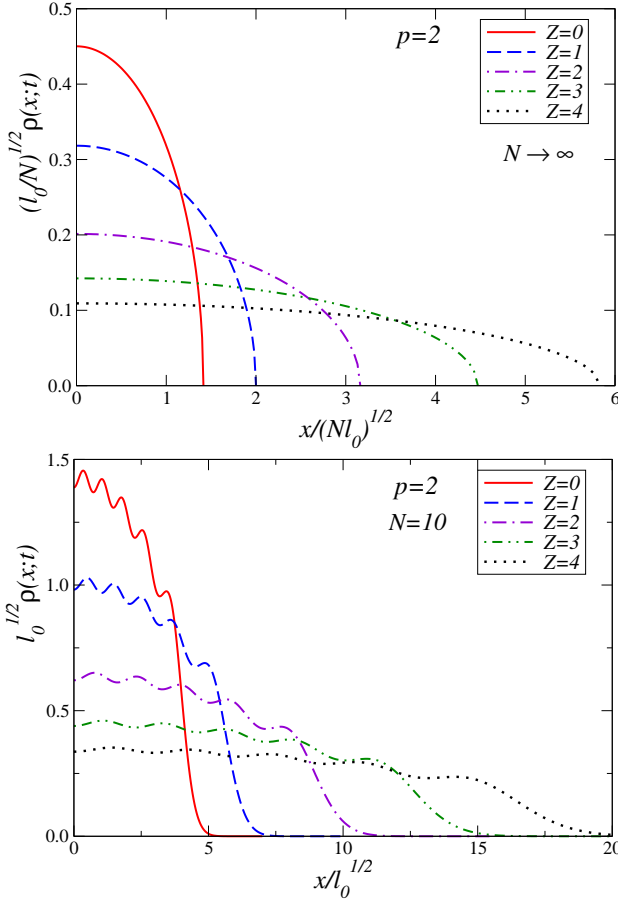


FIG. 15: (Color online) $l_0^\theta \rho(x; t)$ for some values of $Z \equiv l_0^{-2\theta} t$, for $N = 10$ (below) and in the limit $N \rightarrow \infty$ (above), in the case of a quench to the unconfined Hamiltonian.

where $\mathcal{D}_N(X)$ can be derived from Eqs. (40) and (46). Analogously, one can derive the particle-density correlation G_n , cf. Eq. (66), obtaining

$$G_n(x, y; t) = l_0^{-2\theta} Q^{-2} \mathcal{G}_N(X/Q, Y/Q). \quad (115)$$

Results for the particle density and the one-particle density matrix are shown in Figs. 15 and 16.

In the case of a quench to a larger trap size $l_f > l_0$, replacing Eq. (103) into Eq. (100), we again obtain the expression (113), but

$$Q(Z) = \sqrt{1 + (r^2 - 1) [\sin(Z/r)]^2}, \quad (116)$$

where $r \equiv l_f/l_0$. Therefore, we have a periodic time evolution with period $Z_p = r\pi$. Fig. 17 shows results for the periodic time evolution of the particle density for $N = 10$ and $r = 2$.

For a large number of particles in a harmonic potential, we can derive the TSS using the asymptotic behavior given by Eqs. (B1) and (B2). We obtain

$$l_0^\theta \rho(x; t) \approx \frac{(2N)^{1/2}}{\pi Q} \sqrt{1 - \frac{X^2}{2NQ^2}}. \quad (117)$$

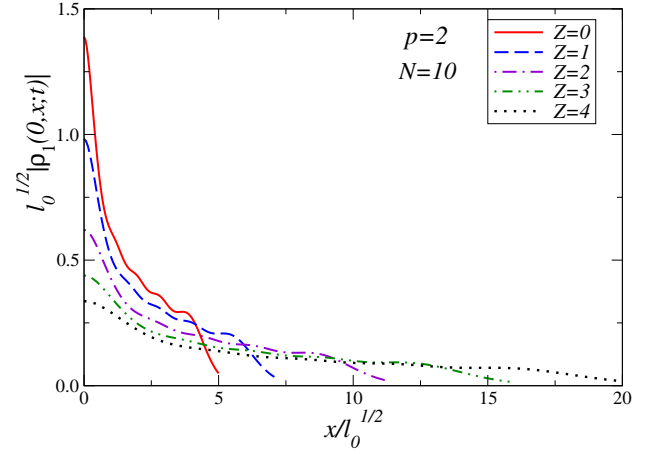


FIG. 16: (Color online) $l_0^\theta |\rho_1(0, x; t)|$ for some values of $Z \equiv l_0^{-2\theta} t$, for $N = 10$ and in the case of a quench to the unconfined Hamiltonian.

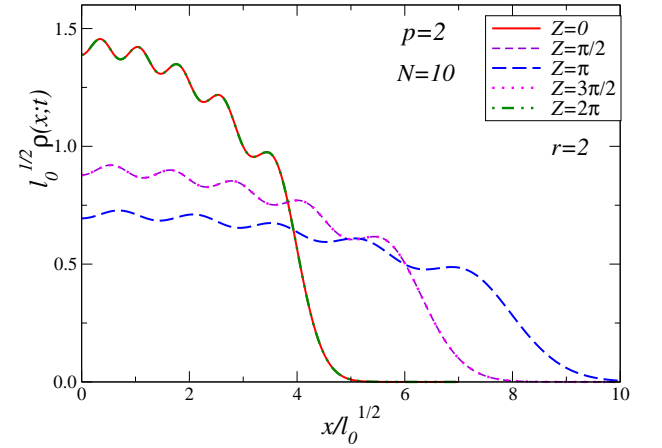


FIG. 17: (Color online) Time dependence of the rescaled particle density $l_0^\theta \rho(x; t)$ for some values of $Z \equiv l_0^{-2\theta} t$, for $N = 10$ and in the case of a quench to a trap with size $l_f = 2l_0$. It oscillates between the $Z = 0$ and $Z = \pi$ curves.

The above results show that, after instantaneous changes of the trap size of the harmonic confining potential, the trap-size dependence satisfies the scaling Ansatz put forward in Sec. V A

It is worth noting that the time-dependence of the particle density $\rho(x; t)$ and its correlation $G_n(x, y; t)$ can be reexpressed as their equilibrium TSS with an effective time-dependent trap size

$$\tilde{l}(t) = l_0 s(t)^{1/\theta} = l_0 Q(Z)^{1/\theta}, \quad (118)$$

so that

$$\rho(x; t) = \tilde{l}(t)^{-\theta} \mathcal{D}_N(\tilde{X}), \quad \tilde{X} \equiv x/\tilde{l}(t)^\theta. \quad (119)$$

We finally mention that the case of a gas of impenetrable bosons in a hard-wall trap, and its expansion after the drop of the trap, was considered in Refs [71, 72]. A hard-wall trap of size L corresponds to the $p \rightarrow \infty$ limit

of the confining potential, cf. Eq. (2), with trap size $l = L/2$. One can easily check that the time evolution of the particle density after the drop of the trap, computed in Ref. [72], is consistent with the scaling Ansatz (69) taking into account that the $p \rightarrow \infty$ limit of the trap exponent (10) is $\theta = 1$ and $l_0 = L/2$.

C. Power-law time dependence of the trapping potential

We now consider the case of a power-law time dependence of the confining potential, cf. Eq. (93).

Let us define the quantities

$$S(Z) \equiv l_0^{q\theta_0/2} s(t), \quad Z \equiv l_0^{-2\theta_0} \tau, \quad (120)$$

where

$$\theta_0 = \frac{1}{2+q} \quad (121)$$

is the off-equilibrium trap exponent obtained by replacing $z = 2$ and $p = 2$ in Eq. (71). $S(Z)$ satisfies the equation

$$S'' + Z^q S = S^{-3} \quad (122)$$

where $S'' \equiv \partial_Z^2 S$. Then, using the equilibrium relation (110), we rewrite Eq. (100) as

$$\begin{aligned} \rho_1(x, y; t) &= l_0^{-\theta_0} S^{-1} \times \\ &\times \mathcal{M}_N(X/S, Y/S) \times \exp \left[i \frac{S'}{2S} (Y^2 - X^2) \right], \end{aligned} \quad (123)$$

where $X = x/l_0^{\theta_0}$, $Y = y/l_0^{\theta_0}$, and \mathcal{M}_N is the same scaling function appearing in Eq. (67).

The evolution of the particle density is easily obtained:

$$\rho(x; t) = \rho_1(x, x; t) = l_0^{-\theta_0} S^{-1} \mathcal{D}_N(X/S), \quad (124)$$

where \mathcal{D}_N is the scaling function (46). For a large number of particles we can derive the off-equilibrium TSS using the asymptotic behavior given by Eqs. (B1) and (B2). We obtain

$$l_0^{\theta_0} \rho(x; t) \approx \frac{(2N)^{1/2}}{\pi S} \sqrt{1 - \frac{X^2}{2NS^2}}. \quad (125)$$

The time dependence of $\rho(x; t)$ can be again reexpressed using the equilibrium expression with an effective trap size

$$\tilde{l}(t) = l_0^{\theta_0/\theta} S^{1/\theta} = l_0 s(t)^{1/\theta}. \quad (126)$$

The function $\tilde{l}(t)$ increases monotonically with decreasing $t < 0$. If one prefers to invert the time evolution, so that the effective trap size increases with increasing $t \geq 0$, it is sufficient to redefine $\tau = 1 - t$ in Eqs. (94) and (104). Note that $\tilde{l}(t)$ remains finite for $\tau = 0$, i.e., when the external potential (93) vanishes, indeed $s(\tau = 0) \simeq 1.14313$, then

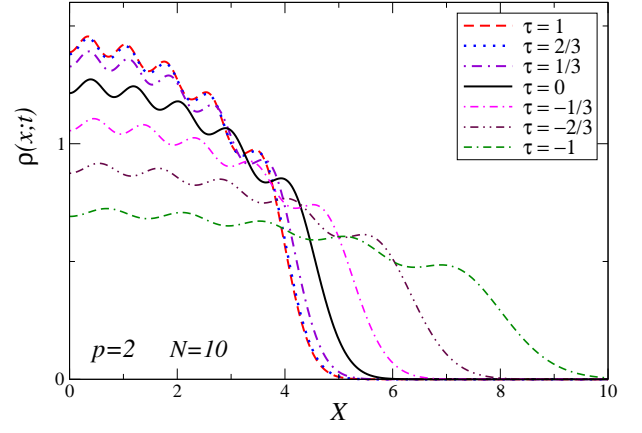


FIG. 18: (Color online) Time dependence of the particle density for $N = 10$ in a time-dependent trap with $\kappa(t) = \tau$, corresponding to $l_0 = 1$.

it diverges in the limit $\tau \rightarrow -\infty$ (note that for $\tau < 0$ and $q = 1$ the potential (93) changes sign, so it does not trap the particles anymore).

The above scaling behaviors are apparently consistent with those predicted by the scaling arguments of Sec. V B for the off-equilibrium TSS in the low-density regime. However, the function $S(Z)$ maintains a residual dependence on l_0 , beside on Z , due to the initial condition of $s(t)$ which corresponds to $l_0^{-q\theta_0/2} S(l_0^{-2\theta_0}) = 1$. Thus, the scaling Ansatz can be actually considered as fully verified only if the function $S(Z)$ has a nontrivial scaling limit for $l_0 \rightarrow \infty$.

In the case of a linear time-dependence of $\kappa(t)$, i.e., $\kappa(t) = \kappa_0 \tau$, the function $S(Z)$ can be derived from the corresponding solution $s(t)$, cf. Eq. (104). Then, using the equilibrium results of Sec. IV, we obtain the time dependence of the one-particle density matrix, the particle density, particle density correlators, momentum distribution, etc.... Some results for the particle density and one-particle density matrix are respectively shown in Figs. 18 and 19.

An important remark is in order. The analytical solution in the case of a linear time dependence shows that the function $S(Z)$ does not have a nontrivial scaling limit for $l_0 \rightarrow \infty$, indeed it appears to diverge, roughly as $(\ln l_0)^2$ at fixed Z . This may reflect the fact that the initial conditions are somehow weakly relevant, leaving a residual weak (logarithmic) dependence in the large- l_0 limit. We should further note that $\tilde{S}(Z) \equiv s(t)$ with $Z \equiv l_0^{-2\theta_0} \tau$ (with $\tau = 1 + t$) has a nontrivial $l_0 \rightarrow \infty$ limit satisfying the differential equation $S'' + ZS = 0$. But this rescaling would not fit any scaling behavior consistent with the dynamic exponent $z = 2$. This point deserves further investigation.

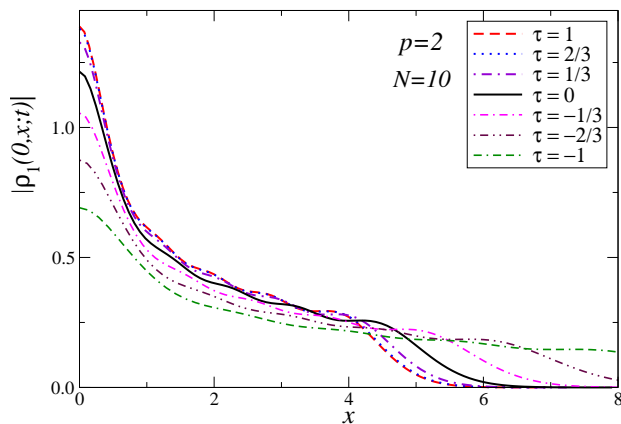


FIG. 19: (Color online) Time dependence of the absolute value of the one-particle density matrix for $N = 10$ in a time-dependent trap with $\kappa(t) = \tau$, corresponding to $l_0 = 1$.

VIII. SUMMARY AND CONCLUSIONS

We study the trap-size dependence of the quantum behavior of dilute gases of bosonic particles in the presence of a confining potential trapping the particles within a limited spatial region. We consider systems of bosonic particles constrained in an optical lattice, described by the Bose-Hubbard (BH) model in the presence of a confining potential coupled to the particle density, cf. Eq. (1). In the case of a harmonic potential $V(x) = v^2 x^2/2$, the corresponding trap size is defined as $l = \sqrt{J}/v$ where J is the hopping parameter. We consider systems at equilibrium and off equilibrium during the unitary time evolution arising from changes of the trapping potential, at zero temperature, i.e., at a sufficient low temperature to neglect its effects. We investigate the trap-size dependence in the low-density regime using the framework of the trap-size scaling (TSS) theory [25, 59].

Using scaling arguments, we infer the power-law trap-size dependence of observables related to the equilibrium lowest states of a dilute gas of N particles in the low-density regime. The low-density regime of the BH model (1), i.e., $Na^d/l^d \ll 1$ where a is the lattice spacing, can be seen as the critical regime of a quantum transition from low density to the empty state, which may be considered as a $n = 0$ Mott transition. Mott transitions driven by the chemical potential are described by the *nonrelativistic* Φ^4 continuum theory (9), where the dynamic exponent is $z = 2$ and the RG dimension of the chemical potential is $y_\mu = 2$, in one and two spatial dimensions. In the presence of a confining potential, the power-law trap-size dependence is described by the equilibrium trap exponent [25, 55] $\theta = p/(p + 2)$ where p is the power of the confining potential. This allows us to derive the universal scaling features of the asymptotic power-law trap-size dependence keeping fixed the particle number N . For a generic observable, whose low-density

critical behavior is described by the RG dimension y_o in the homogeneous system, we obtain the scaling Ansatz $\langle O \rangle_N(l, x) \approx l^{-y_o\theta} \mathcal{O}_N(xl^{-\theta})$, see Sec. II.

The equilibrium TSS scenario is verified in 1D systems by analytical and numerical calculations. We show analytically that the expected TSS holds in the hard-core (HC) limit $U \rightarrow \infty$ of the BH model. We compute the scaling functions of some observables, such as the particle density and its correlators, the one-particle density matrix, see Sec. IIIB 2. The universality of the low-density TSS with respect to the on-site repulsion coupling U is supported by numerical calculations at a finite value of U , i.e., $U = 2$, using DMRG methods. We show that the asymptotic TSS of N particles at equilibrium described by the 1D BH model, in the HC limit and at finite U , is identical to that of a 1D gas of impenetrable bosons (Tonks-Girardeau model), with appropriate definitions of the trap size (in the case of harmonic traps the trap sizes are proportional to the inverse frequency in both models). The lattice structure gives rise to subleading $O(l^{-2\theta})$ scaling corrections in the HC limit of the BH model. The approach to the asymptotic behavior is slower at finite values of U , in agreement with the RG arguments which predict subleading $O(l^{-\theta})$ scaling corrections. We argue that the same scenario applies to the Lieb-Liniger model with a finite contact interaction in the low-density regime, i.e., it presents the same universal asymptotic TSS with $O(l^{-\theta})$ scaling corrections.

We investigate the trap-size dependence of the off-equilibrium dynamics due to time-dependent confining potentials, such as $V(r, t) \sim (1 + t/t_q)^q r^p$, or instantaneous changes of the trap size, including the instantaneous drop of the trap. We extend the scaling Ansatz for the trap-size dependence at equilibrium to off-equilibrium quantum evolutions, to describe the TSS with respect to the initial trap size l_0 , see Sec. V. We argue that $\langle O \rangle_N(x; t) \approx l_0^{-y_o\theta} \mathcal{O}_N(xl_0^{-\theta}, tl_0^{-z\theta}, l_f/l_0)$ in the case of an instantaneous change of the trap size from l_0 to l_f . In the case of a power-law time dependence, we introduce an off-equilibrium trap exponent, given by $\theta_0 = 1/(2 + q)$ in the case of a harmonic trapping potential, and put forward the scaling Ansatz $\langle O \rangle_N(x; t) \approx l_0^{-y_o\theta_0} \mathcal{O}_N(xl_0^{-\theta_0}, \tau l_0^{-z\theta_0})$. The above results are expected to be quite general in the dilute regime of 1D bosonic gases, such the lattice BH model and continuous Lieb-Liniger model.

We then analyze the trap-size dependence of the off-equilibrium dynamics of 1D bosonic gases with respect to the initial trap size l_0 , using adiabatic approximations in the case of slow changes of the parameters, and exact solutions of the Schrödinger equation of N impenetrable bosons in time-dependent traps or after instantaneous changes of the trap size. The evolution after instantaneous quenches agrees with the corresponding off-equilibrium Ansatz (68), where the equilibrium trap exponent θ characterizes the power-law dependence on the initial trap size, see Sec. VII B. In the case of a power-law time dependence of the potential, the evolution supports

the scaling Ansatz in terms of the off-equilibrium trap exponent θ_0 , see Sec. VII C. However, in the case of a linear time dependence, for which we have an analytical solution, the simplest Ansatz (73) does not provide a complete description of the asymptotic large- l_0 behavior because the resulting scaling functions maintain a weak logarithmic dependence on l_0 in the large- l_0 limit, demonstrating that the initial conditions are somehow relevant. This point deserves further investigation.

Our results are of experimental relevance for systems of cold atomic gases trapped by a confining potential. Indeed, the easy tunability and long characteristic time scales of these systems may allow a careful study of the trap-size dependence of the zero-temperature properties of N -particle boson gases, in the continuum and on optical lattices, at equilibrium and off equilibrium in a time-dependent confining potential.

Helpful discussions with P. Calabrese, D. Giuliano, M. Mintchev and G. Morchio are gratefully acknowledged.

Appendix A: TSS in traps induced by a spatial dependence of the hopping parameter

As suggested in Ref. [73], ultracold atomic systems in optical lattices may be also get trapped by appropriate spatially inhomogeneous hopping parameters in the BH model. An example is given by the model

$$\mathcal{H}_{t_{ij}} = -\frac{J}{2} \sum_{\langle ij \rangle} \frac{t_{ij}}{2} (b_j^\dagger b_i + b_i^\dagger b_j) + \frac{U}{2} \sum_i n_i(n_i - 1) \quad (\text{A1})$$

with

$$t_{ij} \equiv h(x_{ij}), \quad x_{ij} = \frac{x_i + x_j}{2}, \quad (\text{A2})$$

$$h(x) = \left[1 + \frac{1}{p} (x/l)^p \right]^{-1},$$

and x_i are the positions of the sites of the lattice. The rescaled hopping parameter t_{ij} tends to one at the middle of the trap and vanishes at large distance, giving rise to an effective trap, with trap size l .

In the HC $U \rightarrow \infty$ limit, the Hamiltonian can be diagonalized exploiting the fermion quadratic representation (22) with

$$h_{ij} = \delta_{ij} - \frac{1}{2} t_{ij} (\delta_{i,j-1} + \delta_{i,j+1}) \quad (\text{A3})$$

following the procedure outlined in Sec. III B 1, cf. Eqs. (32), (33) and (34).

In the dilute region, i.e., for sufficiently small N/l , we can follow the same steps of Sec. III B 1 to arrive at a continuum TSS limit. We end up with the same Schrödinger-like equation (39) after the same rescalings (36), (37) and (38) and $\theta = p/(p+2)$ as well. Thus, the TSS arising from the spatial-inhomogeneity of the hopping parameter, like Eq. (A2), is identical to that of model (1), i.e., of a trap

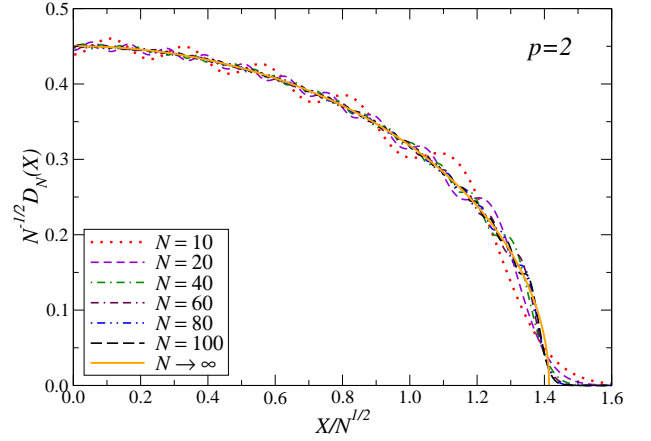


FIG. 20: (Color online) The large- N behavior of $\mathcal{D}_N(X)$ for $p = 2$. The full line shows its $N \rightarrow \infty$ limit, cf. Eq. (B2)

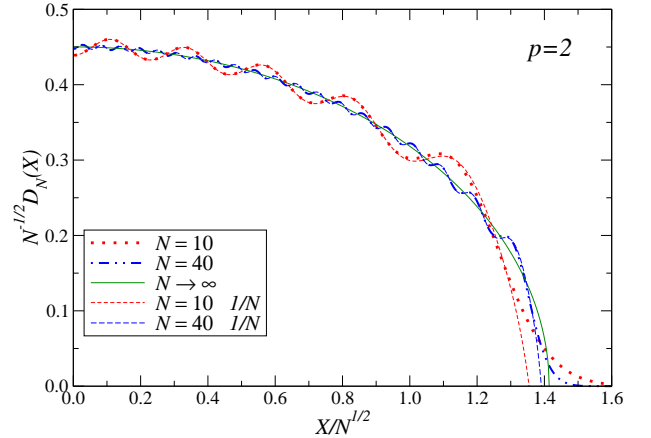


FIG. 21: (Color online) Comparisons of $\mathcal{D}_N(X)$ for $p = 2$ and $N = 10$ and $N = 40$ with their next-to-leading approximations, cf. Eq. (B3), denoted by “ $1/N$ ” in the figure.

achieved by coupling an external potential to the particle density. One can also infer that scaling corrections are $O(l^{-2\theta})$ as well.

Appendix B: Trap-size scaling for a large number of particles

In this appendix we determine the large- N behavior of the TSS functions of the observables considered in Sec. III B 2.

1. The large- N behavior of the TSS functions

In the case of the harmonic potential, the rescaled particle density, cf. Eq. (46), behaves as

$$\mathcal{D}_N(X) = N^{1/2} \left[R_D(\tilde{X}) + \frac{C_D(\tilde{X})}{N} + O(1/N^2) \right], \quad (\text{B1})$$

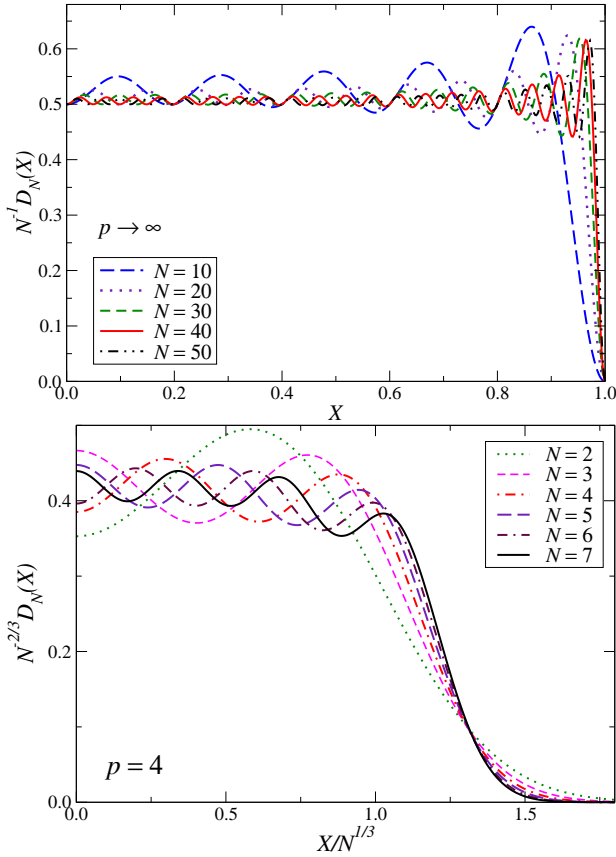


FIG. 22: (Color online) The scaling functions $\mathcal{D}_N(X)$, cf. Eq. (45), for $p = 4$ (below) and $p \rightarrow \infty$ (above).

where $\tilde{X} \equiv N^{-1/2}X$. The approach to the large- N behavior is shown in Fig. 20, where $N^{-1/2}D_N(X)$ is plotted versus \tilde{X} for several values of N . The leading large- N behavior is

$$R_D(x) = \frac{1}{\pi} \sqrt{2 - x^2}, \quad (\text{B2})$$

for $x \leq \sqrt{2}$, and $R_D(x) = 0$ for $x > \sqrt{2}$. This is also the $N \rightarrow \infty$ limit of the particle density in a bosonic gas of impenetrable bosons [41, 50]. Actually, since the low-density limit of the HC-BH model matches the behavior of a gas of impenetrable bosons, as discussed in Sec. IV, we can use results obtained for the TG gas [41] to infer that

$$C_D(x) = -\frac{(-1)^N \cos[Nq(x)]}{\pi \sqrt{2}(2 - x^2)}, \quad (\text{B3})$$

$$q(x) = x\sqrt{2 - x^2} + 2\arcsin(x/\sqrt{2}).$$

A comparison of $\mathcal{D}_N(X)$ for $N = 10$ and $N = 40$ with their next-to-leading large- N approximations is shown in Fig. 21.

Analogous results can be derived for other power laws of the confining potential. Results for $p = 4$ and $p \rightarrow \infty$ are shown in Fig. 22. The particle-density scaling functions show again N peaks, with an underlying structure

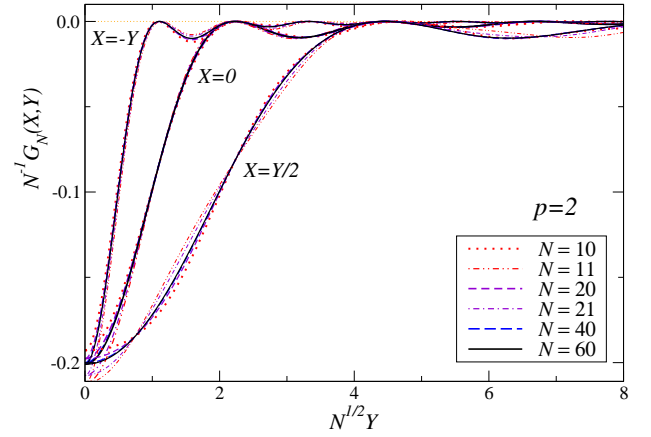


FIG. 23: (Color online) Plot of $N^{-1}\mathcal{G}_N(X, Y)$ for $X = Y/2$, $X = 0$, and $X = -Y$, vs $N^{1/2}Y$, for several values of N . They approach unique curves with increasing N . Even and odd values of N converge from opposite sides.

scaling as $\mathcal{D}_N(X) \approx N^{2/3}R_D(X/N^{1/3})$ for $p = 4$ and $\mathcal{D}_N(X) = N/2 + O(1)$ for $p \rightarrow \infty$ (at least not too close to $X = 1$), with the oscillatory terms suppressed by $1/N$ with respect to the leading terms. These results suggest the general behavior

$$\mathcal{D}_N(X) = N^\theta [R_D(X/N^{1-\theta}) + O(1/N)] \quad (\text{B4})$$

for any power p , where the function R_D depends on p .

Fig. 23 shows results for the scaling function $\mathcal{G}_N(X, Y)$ associated with the density-particle correlation, cf. Eq. (17), for several values of N , obtained from Eq. (48) for the harmonic potential. These plots show that the large- N behavior is

$$\mathcal{G}_N(X, Y) \approx NR_G(N^{1/2}X, N^{1/2}Y) \quad (\text{B5})$$

Note the different N -rescaling of the spatial coordinates with respect to that of the particle density.

Concerning the one-particle density matrix, cf. Eq. (13), we note that the scaling behaviors (B4) and (52), of the particle density and the momentum distribution respectively, can be both derived from the following nontrivial large- N scaling behavior of the one-particle density matrix:

$$\rho_1(x, y) \approx (N/l)^\theta B[N^{-1+\theta}X, N^\theta(Y - X)], \quad (\text{B6})$$

where B is a scaling function, $X = x/l^\theta$ and $Y = y/l^\theta$ (note the different power of N in the two arguments of the function B ; in the case of a harmonic potential they are $N^{-1/2}X$ and $N^{1/2}(Y - X)$ respectively). The above scaling behavior would imply that, with increasing N , the region where the diagonal component is significantly nonzero increases as $N^{1-\theta}$, while the width around it decreases as $N^{-\theta}$. The approach to this large- N limit is generally characterized by $O(N^{-1/2})$ oscillating corrections in the case of the harmonic potential.

2. Power-law behavior at the boundaries where the particle-density vanishes

In this section we discuss the asymptotic large- N power-law behavior at the boundaries of the trap where the particle density is suppressed.

The large- N asymptotic behavior found in App. B holds for $\tilde{X} \equiv N^{-1/2}X < \tilde{X}_c$ where $\tilde{X}_c = \sqrt{2}$ is the value where $R_D(\tilde{X}) = 0$, which is the point around which the particle density vanishes in the large- N limit. However, around the spatial points corresponding to \tilde{X}_c another power law behavior sets, as suggested by the behavior around \tilde{X}_c of the curves shown in Fig. 21. This fact was already noted within the Gaussian unitary ensembles of random matrices [50, 74], whose eigenvalue density corresponds to the particle density in harmonically trapped systems of impenetrable bosons. An analogous change of power law is observed at fixed chemical potential, thus $N \sim l$, at the boundaries of the trap [55].

This phenomenon is related to a *real-space transition* between the low-density particle regime, for $\tilde{X} \lesssim \tilde{X}_c$, and the empty state for $\tilde{X} > \tilde{X}_c$, which occurs at the points x_c corresponding to \tilde{X}_c . Thus we expect that the region around $x = x_c$ develops *critical* modes related to a low-density Mott transition. The effective external potential at x_c can be obtained by expanding the trapping potential around x_c , thus obtaining an approximately linear potential $V_l(x) \sim x - x_c$. Around x_c , other critical modes develop with length scale $\xi \sim l^\sigma$, where σ is the exponent associated with a linear external potential. The value of σ can be inferred by RG arguments analogous to those leading to the determination of the trap exponent θ at the low-density Mott transition [25, 55], which give $\sigma = 1/3$.⁶ For example, this implies that

$$\tilde{X}_c - \tilde{X}_{\max} \sim N^{-2/3} \quad (\text{B7})$$

where \tilde{X}_{\max} corresponds to the abscissa of the rightmost maximum of $\mathcal{D}_N(X)$. More generally, we have the scaling behavior

$$\lim_{N \rightarrow \infty} N^{-1/6} \mathcal{D}_N[N^{1/2}(\tilde{X}_c + N^{-2/3}z)] = f(z). \quad (\text{B8})$$

The scaling function $f(z)$ can be obtained from related computations within the Gaussian unitary ensembles of random matrices [50, 74]:

$$f(z) = 2^{1/2} |\text{Ai}'(2^{1/2}z)|^2 - 2z |\text{Ai}(2^{1/2}z)|^2. \quad (\text{B9})$$

Fig. 24 shows that the above asymptotic behavior is rapidly approached in the large- N limit.

⁶ The exponent σ can be determined by a RG analysis of the perturbation corresponding to a linear potential $V_l(x) = ux$, i.e., $\int d^d x dt V_l(x) |\phi(x)|^2$, at the fixed point of the continuous theory describing the Mott transition [21]. The exponent σ is related to the RG dimension y_u of the parameter u , which can be obtained from the relations $y_u - 1 = d + z - y_{|\phi|^2} = y_\mu = 2$, thus $y_u = 3$, and therefore $\sigma \equiv 1/y_u = 1/3$ for $d = 1$ and $d = 2$.

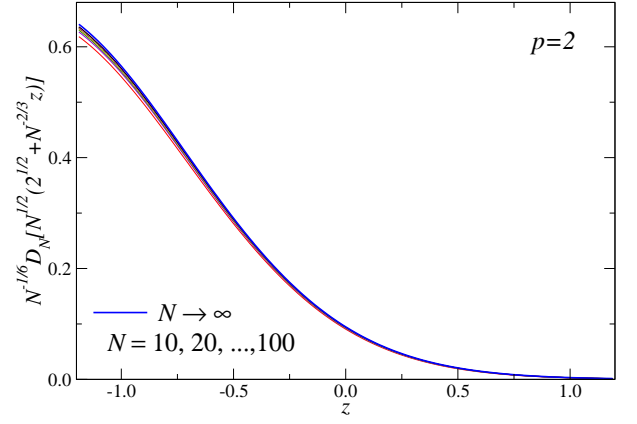


FIG. 24: (Color online) Plot of $N^{-1/6} \mathcal{D}_N[N^{1/2}(\tilde{X}_c + N^{-2/3}z)]$ versus z for $p = 2$, where $\tilde{X}_c = 2^{1/2}$, for $N = 10, 20, \dots, 100$. The curves appear to converge toward the $N \rightarrow \infty$ limit (B9).

Appendix C: The quantum oscillator with a time-dependent frequency

Let us consider a quantum oscillator described by the Hamiltonian

$$H = \frac{p^2}{2} + \kappa(t) \frac{x^2}{2} \quad (\text{C1})$$

with a time dependent frequency

$$\kappa(t) = \omega_0^2 (1 + t/t_q)^q \equiv \omega_0^2 \tau^q, \quad (\text{C2})$$

where t_q is the time rate of the time dependence. In the following we set $t_q = 1$ for simplicity; its dependence can be easily inferred by appropriate rescalings of the results. We assume that at $t = 0$ the oscillator is in its ground state, i.e., its wave function is

$$\psi_0(x) = (\omega_0/\pi)^{1/4} e^{-\omega_0 x^2/2}. \quad (\text{C3})$$

The evolution equation

$$i\partial_t \psi(x, t) = H\psi(x, t) \quad (\text{C4})$$

with $\psi(x, 0) = \psi_0(x)$ preserves the Gaussian spatial dependence. We write the solution of Eq. (C4) as

$$\psi(x, t) = (\omega_0/\pi)^{1/4} e^{-w(t)\omega_0 x^2/2 + z(t)}, \quad (\text{C5})$$

where $w(t)$ and $z(t)$ satisfy the equations

$$\begin{aligned} i\dot{w} &= \omega_0(w^2 - \tau^q), \\ i\dot{z} &= \omega_0 w/2, \end{aligned} \quad (\text{C6})$$

with initial conditions $w(0) = 1$ and $z(0) = 0$. In the case of a linear dependence of κ , i.e.,

$$\kappa(t) = 1 + t \equiv \tau, \quad (\text{C7})$$

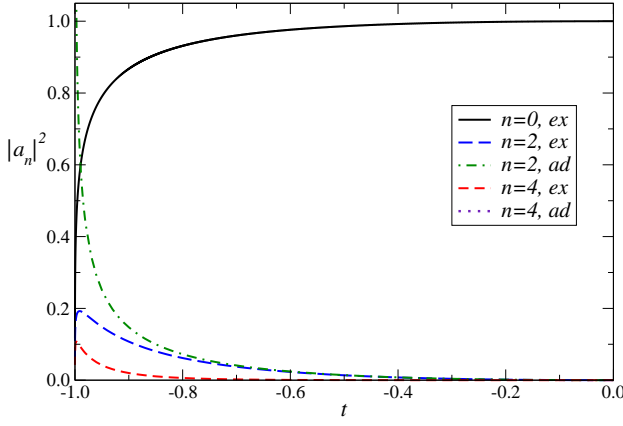


FIG. 25: (Color online) Some results for the coefficients of the expansion (C9) versus t , using exact results from Eq. (C11) and from the adiabatic approximation (C12).

the solution is $w(t) = W(\tau)$ where $W(\tau)$ is the complex function given in Eq. (106), and

$$z(t) = -\frac{i\omega_0}{2} \int_0^t dt' w(t'). \quad (\text{C8})$$

Note that $\psi(x, t)$ remains exponentially suppressed at large x even at $t = -1$ when $\kappa = 0$, indeed $w(-1)|_{\omega_0=1} = W(0)|_{\omega_0=1} = 0.765265 + i0.346358$.

It is interesting to compare the exact solution (C5) with the evolution predicted by the adiabatic perturbation theory. In the following calculations we set $\omega_0 = 1$. We expand the wave function as

$$\psi(x, t) = \sum_n a_n(t) \phi_n(x, t), \quad (\text{C9})$$

where $\sum_n |a_n(t)|^2 = 1$ and $\phi_n(x, t)$ are *instantaneous* eigenstates, i.e.,

$$\begin{aligned} H\phi_n(x, t) &= E_n(t)\phi_n(x, t), \\ E_n &= \omega(t)(n + 1/2), \quad \omega(t) = \sqrt{\kappa(t)}, \\ \phi_n(x, t) &= \frac{1}{\pi^{1/4}(2^n n!)^{1/2}} H_n[x\omega(t)^{1/2}] e^{-\omega(t)x^2/2}, \end{aligned} \quad (\text{C10})$$

where $H_n(x)$ are the Hermite polynomials. The coefficients $a_n(t)$ are given by

$$a_n(t) = \int dx \psi(x, t)^* \phi_n(x, t). \quad (\text{C11})$$

Note that $a_n = 0$ for odd values of n (when the corresponding eigenfunction ϕ_n is odd). Moreover, $a_n(t) \rightarrow 0$ for $t \rightarrow -1$.

Assuming a very slow variation of the Hamiltonian parameters, we expect an adiabatic evolution, i.e., the system starting from the ground state at $t = 0$ evolves through the *instantaneous* ground states $\phi_0(x, t)$. Thus, the leading behavior is given by $a_n(t) = e^{i\Theta_n(t)} \delta_{n0}$ where $\Theta_n(t) = \int_0^t E_n(t) dt$. The time dependent coefficients $a_n(t)$ can be computed to the next-to-leading order of the adiabatic perturbative expansion, see, e.g., Refs. [68, 69], obtaining

$$a_n(t) = -e^{i\Theta_n(t)} \int_0^t dt' \frac{\langle n | \partial_t H | 0 \rangle}{E_n(t') - E_0(t')} e^{-i\Delta\Theta_{n0}(t')} \quad (\text{C12})$$

where $\Delta\Theta_{nm} \equiv \Theta_n - \Theta_m$. Beside $a_0(t)$, only the coefficient $a_2(t)$ differs from zero in the first order adiabatic approximation. Note that the limit $t \rightarrow -1$, thus $\tau \rightarrow 0$, is singular; indeed $|a_2(t)| \sim |\ln \tau|$. This shows that the adiabatic approximation fails approaching the *critical* point where the spectrum tends to become degenerate.

Some results for the coefficients $a_n(t)$ are shown in Fig. 25, as obtained from Eq. (C11) and their adiabatic approximation. We find that $|a_0(t)|^2 \gtrsim 0.99$ for $\tau \equiv 1 + t \gtrsim 0.5$, which is the region where the zero-order adiabatic approximation works within 1%, and $|a_0(t)|^2 + |a_2(t)|^2 \gtrsim 0.99$ for $\tau \gtrsim 0.2$, which is where the first-order adiabatic approximation is effective.

[1] E.A. Cornell and C.E. Wieman, Rev. Mod. Phys. 74, 875 (2002); N. Ketterle, Rev. Mod. Phys. 74, 1131 (2002).
[2] I. Bloch, J. Dalibard, and W. Zwerger, Rev. Mod. Phys. 80, 885 (2008).
[3] Z. Hadzibabic, P. Krüger, M. Cheneau, B. Battelier, and J. Dalibard, Nature 441, 1118 (2006).
[4] T. Donner, S. Ritter, T. Bourdel, A. Öttl, M. Köhl, and T. Esslinger, Science 315, 1556 (2007).
[5] P. Cladé, C. Ryu, A. Ramanathan, K. Helmerson, and W.D. Phillips, Phys. Rev. Lett. 102, 170401 (2009).
[6] M. Greiner, I. Bloch, M.O. Mandell, T. Hänsch, and T. Esslinger, Nature 415, 39 (2002).

[7] T. Kinoshita, T. Wenger, and D.S. Weiss, Science 305, 1125 (2004); Phys. Rev. Lett. 95, 190406 (2005).
[8] S. Fölling, A. Widera, T. Müller, F. Gerbier, and I. Bloch, Phys. Rev. Lett. 97, 060403 (2006).
[9] I.B. Spielman, W.D. Phillips, and J.V. Porto, Phys. Rev. Lett. 98, 080404 (2007); Phys. Rev. Lett. 100, 120402 (2008).
[10] D. Clément, N. Fabbri, L. Fallani, C. Fort, and M. Inguscio, Phys. Rev. Lett. 102, 155301 (2009).
[11] O. Morsch, D. Ciampini, and E. Arimondo, Europhys. Lett. 41/3, 21 (2010).
[12] M. Greiner, O. Mandel, T.W. Hänsch, and I. Bloch, Na-

- ture 419, 51 (2002).
- [13] T. Kinoshita, T. Wenger, and D.S. Weiss, *Nature* 440, 900 (2006).
 - [14] L.E. Sadler, M. Higbie, S.R. Leslie, M. Vengalattore, and D.M. Stamper-Kurn, *Nature* 443, 312 (2006).
 - [15] T. Kinoshita, T. Wenger, and D.S. Weiss, *Science* 305, 1125 (2004); *Phys. Rev. Lett.* 95, 190406 (2005).
 - [16] T. Stöferle, H. Moritz, C. Schori, M. Köhl, and T. Esslinger, *Phys. Rev. Lett.* 92, 130403 (2004).
 - [17] B. Paredes, A. Widera, V. Murg, O. Mandel, S. Fölling, I. Cirac, G. Shlyapnikov, R.W. Hänsch, and I. Bloch, *Nature* 429, 277 (2004).
 - [18] B. Laburthe Tolra, K.M. O'Hara, J.H. Huckans, W.D. Phillips, S.L. Rolston, and J.V. Porto, *Phys. Rev. Lett.* 92, 190401 (2004).
 - [19] S. Hofferberth, I. Lesanovsky, B. Fischer, T. Schumm, and J. Schmiedmayer, *Nature* 449, 324 (2007).
 - [20] D. Jaksch, C. Bruder, J.I. Cirac, C.W. Gardiner, and P. Zoller, *Phys. Rev. Lett.* 81, 3108 (1998).
 - [21] M.P.A. Fisher, P.B. Weichman, G. Grinstein, and D.S. Fisher, *Phys. Rev. B* 40, 546 (1989).
 - [22] V. Bretin, S. Stock, Y. Seurin, and J. Dalibard, *Phys. Rev. Lett.* 92, 050403 (2004).
 - [23] S. Sachdev, *Quantum Phase Transitions* (Cambridge Univ. Press, 1999).
 - [24] M. Rigol and A. Muramatsu, *Phys. Rev. A* 70, 031603 (2004); *Phys. Rev. A* 72, 013604 (2005).
 - [25] M. Campostrini and E. Vicari, *Phys. Rev. A* 81, 023606 (2010); *J. Stat. Mech.: Theory Exp.* P08020 (2010).
 - [26] D.S. Petrov, D.M. Gangardt, and G.V. Shlyapnikov, *J. Phys. IV France* 116, 3-44 (2004).
 - [27] E.H. Lieb and W. Liniger, *Phys. Rev.* 130, 1605 (1963); E.H. Lieb, *Phys. Rev.* 130, 1616 (1963).
 - [28] M. Girardeau, *J. Math. Phys. (N.Y.)* 1, 516 (1960).
 - [29] M.D. Girardeau, *Phys. Rev.* 139, B500 (1965).
 - [30] D.S. Petrov, G.V. Shlyapnikov, and J.T.M. Walraven, *Phys. Rev. Lett.* 85, 3745 (2000).
 - [31] Yu. Kagan, E.L. Surkov, and G.V. Shlyapnikov, *Phys. Rev. A* 54, R1753 (1996).
 - [32] M.D. Girardeau and E.M. Wright, *Phys. Rev. Lett.* 84, 5691 (2000).
 - [33] E.B. Kolomeisky, T.J. Newman, J.P. Straley, and Xiaoya Qi, *Phys. Rev. Lett.* 85, 1146 (2000).
 - [34] V. Dunjko, V. Lorent, and M. Olshanii, *Phys. Rev. Lett.* 86, 5413 (2001).
 - [35] M.D. Girardeau, E.M. Wright, and J.M. Triscari, *Phys. Rev. A* 63, 033601 (2001).
 - [36] G.J. Lapeyre, M.D. Girardeau, and E.M. Wright, *Phys. Rev. A* 66, 23606 (2002).
 - [37] G.G. Batrouni, V. Rousseau, R.T. Scalettar, M. Rigol, A. Muramatsu, P.J.H. Denteneer, and M. Troyer, *Phys. Rev. Lett.* 89, 117203 (2002).
 - [38] C. Menotti, S. Stringari, *Phys. Rev. A* 66, 043610 (2002).
 - [39] A. Polkovnikov, S. Sachdev, and S.M. Girvin, *Phys. Rev. A* 66, 053607 (2002).
 - [40] P.J. Forrester, N.E. Frankel, T.M. Geroni, and N.S. Witte, *Commun. Math. Phys.* 238, 257 (2003); *Phys. Rev. A* 67, 043607 (2003).
 - [41] F. Kalish and D. Braak, *J. Phys. A* 35, 9957 (2002).
 - [42] T. Papenbrock, *Phys. Rev. A* 67, 041601 (2003).
 - [43] P.J. Forrester, N.E. Frankel, T.M. Geroni, and N.S. Witte, *Phys. Rev. A* 67, 043607 (2003).
 - [44] D.M. Gangardt and G.V. Shlyapnikov, *Phys. Rev. Lett.* 90, 010401 (2003).
 - [45] D.M. Gangardt, *J. Phys. A* 37, 9335 (2004).
 - [46] C. Kollath, U. Schollwöck, J. von Delft, and W. Zwerger, *Phys. Rev. A* 69, 031601 (2004).
 - [47] L. Pollet, S. Rombouts, K. Heyde, and J. Dukelsky, *Phys. Rev. A* 69, 043601 (2004).
 - [48] S. Wessel, F. Alet, M. Troyer, and G.G. Batrouni, *Phys. Rev. A* 70, 053615 (2004).
 - [49] A. Minguzzi and D.M. Gangardt, *Phys. Rev. Lett.* 94, 240404 (2005).
 - [50] T.M. Geroni, P.J. Forrester, and N.E. Frankel, *J. Math. Phys.* 46, 103301 (2005).
 - [51] M. Cramer, C.M. Dawson, J. Eisert, and T.J. Osborne, *Phys. Rev. Lett.* 100, 030602 (2008).
 - [52] A. Polkovnikov and V. Gritsev, *Nature Phys.* 4, 477 (2008).
 - [53] G.G. Batrouni, H.R. Krishnamurthy, K.W. Mahmud, V.G. Rousseau, and R.T. Scalettar, *Phys. Rev. A* 78, 023627 (2008).
 - [54] M. Rigol, G.G. Batrouni, V.G. Rousseau and R.T. Scalettar, *Phys. Rev. A* 79, 053605 (2009).
 - [55] M. Campostrini and E. Vicari, *Phys. Rev. A* 81, 063614 (2010).
 - [56] M. Collura and D. Karevski, *Phys. Rev. Lett.* 104, 200601 (2010).
 - [57] G. Roux, *Phys. Rev. A* 81, 053604 (2010).
 - [58] L. Pollet, N.V. Prokof'ev, and B.V. Svistunov, *Phys. Rev. Lett.* 104, 245705 (2010).
 - [59] M. Campostrini and E. Vicari, *Phys. Rev. Lett.* 102, 240601 (2009).
 - [60] E. Hairer, S.P. Norsett, and G. Wanner, *Solving ordinary differential equations I: Nonstiff problems* (Berlin, New York: Springer-Verlag, 1993).
 - [61] L.D. Landau and E.M. Lifshitz, *Quantum Mechanics: Non-Relativistic Theory*, Vol. 3 (3rd ed.) (Pergamon Press 1977).
 - [62] A. Minguzzi, P. Vignolo, and M.P. Tosi, *Phys. Lett. A* 294, 222 (2002).
 - [63] M. Olshanii and V. Dunjko, *Phys. Rev. Lett.* 91, 090401 (2003).
 - [64] A. Pelissetto and E. Vicari, *Phys. Rep.* 368, 549 (2002).
 - [65] K.G. Wilson, in *Nobel Lectures in Physics 1981-1990*, G. Ekspeng Ed., World Scientific Publ., Singapore, 1993.
 - [66] H.K. Janssen, B. Schaub and B. Schmittmann, *Z. Phys. B* 73, 539 (1989).
 - [67] P. Calabrese and A. Gambassi, *J. Phys. A* 38, R133 (2005).
 - [68] L.I. Schiff, *Quantum Mechanics*, McGraw-Hill Kogakusha, LTD (1977).
 - [69] C. De Grandi and A. Polkovnikov, *Quantum Quenching, Annealing and Computation*, Eds. A. Das, A. Chandra and B. K. Chakrabarti, Lect. Notes in Phys., vol. 802 (Springer, Heidelberg 2010).
 - [70] V.S. Popov and A.M. Perelomov, *Sov. Phys. JETP* 30, 910 (1970); A.M. Perelomov and Y.B. Zel'dovich, *Quantum mechanics* (World Scientific, Singapore, 1998).
 - [71] P. Öhberg, L. Santos, *Phys. Rev. Lett.* 89, 240402 (2002).
 - [72] A. del Campo and J.G. Muga, *Europhys. Lett.* 74, 965 (2006).
 - [73] V.G. Rousseau, G.G. Batrouni, D.E. Sheehy, J. Moreno, and M. Jarrell, *Phys. Rev. Lett.* 104, 167201 (2010).
 - [74] P.J. Forrester, *Nucl. Phys. B* 402, 709 (1993).

